Department of Computer Science, UTSA
Technical Report: CS-TR-2008-005

Reliability-Aware Energy Management for Periodic Real-Time Tasks*

Dakai Zhu
Department of Computer Science
University of Texas at San Antonio
San Antonio, TX, 78249
dzhu@cs.utsa.edu

Hakan Aydin
Department of Computer Science
George Mason University
Fairfax, VA 22030
aydin@cs.gmu.edu

Abstract

Dynamic Voltage and Frequency Scaling (DVFS) has been widely used to manage energy in real-time embedded systems. However, it was recently shown that DVFS has direct and adverse effects on system reliability. In this work, we investigate static and dynamic *reliability-aware energy management* schemes to minimize energy consumption for *periodic* real-time systems while preserving system reliability. Focusing on *earliest deadline first (EDF)* scheduling, we first show that the static version of the problem is NP-hard and propose two *task-level* utilization-based heuristics. Then, we develop a *job-level* online scheme by building on the idea of *wrapper-tasks*, to monitor and manage dynamic slack efficiently in reliability-aware settings. The feasibility of the dynamic scheme is formally proved. Finally, we present two integrated approaches to reclaim both static and dynamic slack at run-time. To preserve system reliability,

*A preliminary version of this paper appeared in IEEE RTAS 2007. This work is supported in part by NSF award CNS-0720651, CNS-0720647 and NSF CAREER Award CNS-0546244.

the proposed schemes incorporate recovery tasks/jobs into the schedule as needed, while still using the remaining slack for energy savings. The proposed schemes are evaluated through extensive simulations. The results confirm that all the proposed schemes can preserve the system reliability and the ordinary (but *reliability-ignorant*) energy management schemes will result in drastically decreased system reliability. For the static heuristics, the energy savings are close to what can be achieved by an optimal solution by a margin of 5%. By effectively exploiting the run-time slack, the dynamic schemes can achieve additional energy savings while preserving system reliability.

1 Introduction

The phenomenal improvements in the performance of computing systems have resulted in drastic increases in power densities. For battery-operated embedded devices with limited energy budget, energy is now considered a first-class system resource. Many hardware and software techniques have been proposed to manage power consumption in modern computing systems and *power aware computing* has recently become an important research area. One common strategy to save energy is to operate the system components at low-performance (thus, low-power) states, whenever possible. For example, *Dynamic Voltage and Frequency Scaling (DVFS)* technique is based on scaling down the CPU supply voltage and processing frequency simultaneously to save energy [34, 35].

For real-time systems where tasks have stringent timing constraints, scaling down the clock frequency (i.e. processing speed) may cause deadline misses and special provisions are needed. In the recent past, several research studies explored the problem of minimizing energy consumption while meeting all the deadlines for various real-time task models. These include a number of power management schemes which exploit the available static and/or dynamic *slack* in the system [4, 11, 27, 30, 31]. For instance, the optimal static power management scheme for a set of periodic tasks would scale down the execution of all tasks uniformly at a speed proportional to the system utilization and employ the *Earliest-Deadline-First (EDF)* scheduling policy [4, 27].

Reliability and fault tolerance have always been major factors in computer system design. Due to the effects of hardware defects, electromagnetic interferences and/or cosmic ray radiations, faults may occur at run-time, especially in systems deployed in dynamic/vulnerable environments. Several research studies reported that the *transient* faults occur much more frequently than the *permanent* faults [9, 21]. With the continued scaling of CMOS technologies and reduced design margins for higher performance, it is expected that, in addition to the systems that operate in electronics-hostile

environments (such as those in outer space), practically all digital computing systems will be remarkably vulnerable to *transient faults* [15].

The *backward error recovery* techniques, which restore the system state to a previous *safe state* and repeat the computation, can be used to tolerate transient faults [29]. It is worth noting that both DVFS and backward recovery techniques are based on (and compete for) the active use of the system slack. Thus, there is an interesting trade-off between energy efficiency and system reliability. Moreover, DVFS has been shown to have a direct and adverse effect on the transient fault rates, especially for those induced by cosmic ray radiations [12, 15, 42], further complicating the problem. Hence, for safety-critical real-time embedded systems (such as satellite and surveillance systems) where reliability is as important as energy efficiency, *reliability-cognizant* energy management becomes a necessity.

Fault tolerance through redundancy and energy management through DVFS have been extensively (but, independently) studied in the context of real-time systems. Only recently, few research groups began to investigate the implications of having both fault tolerance and energy efficiency requirements [14, 26, 33, 36]. However, none of them considers the negative effects of DVFS on system reliability. As the first effort to address the effects of DVFS on transient faults, we have previously studied a *reliability-aware power management (RA-PM)* scheme. The central idea of the scheme is to exploit the available slack to schedule a recovery task at the dispatch time of a task before utilizing the remaining slack for DVFS to save energy, thereby preserving the system reliability [38]. The scheme has been extended to consider various task models and reliability requirements [39, 41, 44, 45].

In this paper, we investigate both static and dynamic RA-PM schemes for a set of periodic real-time tasks scheduled by the preemptive EDF policy. Specifically, we consider the problem of exploiting the system's static and dynamic slack to save energy while preserving system reliability. We show that the optimal static RA-PM problem is *NP-hard* and propose two efficient heuristics for selecting a subset of tasks to use static slack (i.e., spare CPU capacity) for energy and reliability management. Moreover, we develop a *job-level* dynamic RA-PM algorithm that monitors and manages the dynamic slack which may be generated at run-time, again for these dual objectives. The latter algorithm is built on the *wrapper-task* mechanism: the key idea is to *conserve* the dynamic slack allocated to scaled tasks for recovery across preemption points, which is essential for preserving reliability. Integrated schemes for effectively exploiting both static and dynamic slack in a uniform manner are also presented. To the best of our knowledge, this is the first research effort that provides a *comprehensive* energy and reliability management framework for *periodic* real-time

tasks.

The remainder of this paper is organized as follows. The related work is summarized in Section 2. Section 3 presents the system models. Section 4 focuses on the task-level static RA-PM schemes. The *wrapper-task* mechanism and the job-level dynamic RA-PM scheme are studied in Section 5. Section 6 presents the integrated slack reclamation mechanisms. Simulation results are discussed in Section 7 and we conclude in Section 8.

2 Related Work

In [33], Unsal *et al.* proposed a scheme to postpone the execution of backup tasks to minimize the overlap of primary and backup execution and thus, the energy consumption. The optimal number of checkpoints, evenly or unevenly distributed, to achieve minimal energy consumption while tolerating a single fault was explored by Melhem *et al.* in [26]. Elnozahy *et al.* proposed an *Optimistic Triple Modular Redundancy (OTMR)* scheme that reduces the energy consumption for traditional TMR systems by allowing one processing unit to slow down provided that it can catch up and finish the computation before the application deadline [14]. The optimal frequency settings for OTMR was further explored in [43]. Assuming a Poisson fault model, Zhang *et al.* proposed an adaptive checkpointing scheme that dynamically adjusts checkpoint intervals for energy savings while tolerating a fixed number of faults for a single task [36]. The work is further extended to a set of periodic tasks [37].

For the existing DVFS-based research efforts, most of the research either focused on tolerating fixed number of faults [14, 26] or assumed constant fault rate [36, 37]. However, it was shown that there is a direct and negative effect of voltage scaling on the rate of transient faults [12, 15, 42]. Taking such effects into consideration, Ejlali *et al.* studied schemes that combine the information (about hardware resources) and temporal redundancy to save energy and to preserve system reliability [13]. Recently, Pop *et al.* studied the problem of energy and reliability trade-offs for distributed heterogeneous embedded systems [28]. The main idea is to tolerate transient faults by switching to pre-determined contingency schedules and re-executing processes. A novel, constrained logic programming-based algorithm is proposed to determine the voltage levels, process start time and message transmission time to tolerate transient faults and minimize energy consumption while meeting the timing constraints of the application.

In our recent work, to address the problem of reliability degradation under DVFS, we have studied a *reliability-aware power management (RA-PM)* scheme based on a single-task model. The central

idea of RA-PM is to reserve a portion of the available slack to schedule a *recovery task* for the task whose execution is scaled down, to recuperate the reliability loss due to the energy management [38]. The idea has been extended later to consider various task models [39, 44] as well as different reliability requirements [45].

The work reported in this paper is different from all previous work in that, focusing on preemptive EDF scheduling, we study the reliability-aware power management problem for a set of *periodic* real-time tasks, where both task-level static schemes and job-level dynamic schemes are proposed. In addition, integrated approaches with a uniform static and dynamic slack reclamation mechanism are also explored.

3 System Models and Problem Description

3.1 Application Model

We consider a set of independent periodic real-time tasks $\Gamma = \{T_1, \ldots, T_n\}$. The task T_i is characterized by the pair (p_i, c_i), where p_i represents its period (which is also the relative deadline) and c_i denotes its worst case execution time (WCET). The first job of each task is assumed to arrive at time 0. The jth *job* of T_i, which is referred to as J_{ij}, arrives at time $(j-1) \cdot p_i$ and has a deadline of $j \cdot p_i$.

In DVFS settings, it is assumed that the WCET c_i of task T_i is given under the maximum processing speed f_{max}. For simplicity, we assume that the execution time of a task scales *linearly* with the processing speed[1]. That is, at the scaled speed f ($\leq f_{max}$), the execution time of task T_i is assumed to be $c_i \cdot \frac{f_{max}}{f}$.

The *system utilization* is defined as $U = \sum_{i=1}^{n} u_i$, where $u_i = \frac{c_i}{p_i}$ is the utilization for task T_i. The tasks are to be executed on a uni-processor system according to the preemptive EDF policy. Considering the well-known feasibility condition for EDF [25], we assume that $U \leq 1$.

3.2 Power Model

The operating frequency for CMOS circuits is almost linearly related to the supply voltage [7]. DVFS reduces supply voltage for lower frequency requirements to save power/energy [34] and, in what follows, we will use the term *frequency change* to stand for both supply voltage and frequency

[1]A number of studies have indicated that the execution time of tasks does not scale linearly with reduced processing speed due to accesses to memory [32] and/or I/O devices [6]. However, exploring the full implications of this observation is beyond the scope of this paper and is left as our future work.

adjustments. Considering the ever-increasing static leakage power due to scaled feature size and increased levels of integration [23], as well as the power-saving states provided in modern power-efficient components (e.g., CPU [2] and memory [24]), in this work, we adopt the simple *system-level power model* proposed in [42] (similar power models have been adopted in several previous work [3, 11, 19, 23, 30]), where the power consumption $P(f)$ of a computing system at frequency f is given by:

$$P(f) = P_s + \hbar(P_{ind} + P_d) = P_s + \hbar(P_{ind} + C_{ef} f^m) \tag{1}$$

Above, P_s is the *static power*, which includes the power to maintain basic circuits and to keep the clock running. It can be removed only by powering off the whole system. P_{ind} is the *frequency-independent active power*, which is a constant and corresponds to the power that is independent of CPU processing speed. It can be efficiently removed (in a couple of cycles) by putting systems into sleep state(s) [2, 24]. P_d is the *frequency-dependent active power*, which includes the processor's dynamic power and *any* power that depends on system processing frequency f (and the corresponding supply voltage) [7, 24].

When there is computation in progress, the system is *active* and $\hbar = 1$. Otherwise, when the system is turned off or in power-saving sleep modes, $\hbar = 0$. The effective switching capacitance C_{ef} and the dynamic power exponent m (in general, $2 \leq m \leq 3$) are system-dependent constants [7]. Despite its simplicity, this power model captures the essential components for system-wide energy management.

Note that, the switching capacitance C_{ef} may be different for different tasks [3, 10, 39]. For simplicity, we assume that C_{ef} is the average system switch capacitance. That is, the value of C_{ef} is the same for different tasks, as in most of the existing work [4, 11, 27, 31, 30]. Instead, we focus in this paper on how to manage energy and reliability simultaneously. However, we would like to emphasize that the RA-PM schemes proposed in this paper can be easily extended to consider the *task dependent* C_{ef} following a similar approach as in our previous work [3, 39].

Moreover, we assume that the *normalized* processing frequency is used with the maximum frequency as $f_{max} = 1$ and the frequency f can be varied continuously from the minimum available frequency f_{min} to f_{max}. The implications of having discrete speed levels are discussed in Section 7.3. In addition, the overhead of frequency adjustment is assumed to be negligible or such overhead can be incorporated into the WCET of tasks.

Minimum energy-efficient frequency: Considering that *energy* is the integral of power over time,

the energy consumption for executing a given job at the constant frequency f will be $E(f) = P(f) \cdot t(f) = P(f) \cdot \frac{c}{f}$, where $t(f) = \frac{c}{f}$ is the execution time of the job at frequency f. From Equation (1), intuitively, lower frequencies result in less frequency-dependent active energy consumption. But with reduced speeds, the job runs longer and thus consumes more static and frequency-independent active energy. Therefore, a minimal *energy-efficient frequency* f_{ee}, below which DVFS starts to consume more total energy, does exist [19, 23, 30]. Considering the prohibitive overhead of turning on/off a system (e.g., tens of seconds), we assume that the system will is on and P_s is always consumed during the operation interval considered (but it can be put into power-saving sleep states). From the above equations, one can find that [42]:

$$f_{ee} = \sqrt[m]{\frac{P_{ind}}{C_{ef} \cdot (m-1)}} \tag{2}$$

Consequently, for energy efficiency, we limit the processing frequency to be $f_{ee} \leq f \leq f_{max}$.

3.3 Fault and Recovery Models

At run-time, faults may occur due to various reasons, such as hardware failures, electromagnetic interferences as well as the effects of cosmic ray radiations. The *transient* faults occur much more frequently than *permanent* faults [9, 21], especially with the continued scaling of CMOS technology sizes and reduced design margins for higher performance [15]. Consequently, in this paper, we focus on transient faults, which in general follow a Poisson distribution [36, 37]. Note that, DVFS has been shown to have a direct and negative effect on system reliability due to increased number of transient faults (especially the ones induced by cosmic ray radiations) at lower supply voltages [12, 15]. Therefore, the average transient fault arrival rate for systems running at scaled frequency f (and corresponding supply voltage) can be expressed as [42]:

$$\lambda(f) = \lambda_0 \cdot g(f) \tag{3}$$

where λ_0 is the average fault rate corresponding to f_{max}. That is, $g(f_{max}) = 1$. With reduced processing speeds and supply voltages, the fault rate generally increases [42]. Therefore, we have $g(f) > 1$ for $f < f_{max}$.

It is assumed that transient faults are detected by using *sanity* (or *consistency*) checks at the completion of a job's execution [29]. When faults are detected, *backward recovery* techniques will be employed for fault tolerance and the recovery task is dispatched, in the form of re-execution

[26, 36, 38]. Again, for simplicity, the overhead for fault detection is assumed to be incorporated into the WCETs of tasks.

3.4 Problem Description

Our primary objective in this paper is to develop power management schemes for periodic real-time tasks executing on a uni-processor system and to preserve system reliability at the same time. The reliability of a real-time system generally depends on the *correct* execution of *all* jobs. Although it is possible to preserve the overall system reliability while sacrificing the reliability for some individual jobs, for simplicity, we focus on maintaining the reliability of *individual* jobs in this work. Here, the *reliability* of a real-time job is defined as the *probability of its being correctly executed (considering the possible recovery, if any) before its deadline*.

Therefore, the problem to be addressed in this paper is, **for a periodic real-time task set with utilization U, how to efficiently use the spare CPU utilization $(1 - U)$, as well as the dynamic slack generated at run-time, in order to maximize energy savings while keeping the reliability of any job of task T_i no less than R_i^0 ($i = 1, \ldots, n$)**, where $R_i^0 = e^{-\lambda_0 c_i}$ (from Poisson fault arrival pattern with the average fault rate λ_0 at f_{max} [38]) represents the *original* reliability for T_i's jobs, when there is no power management and the jobs use their WCETs.

Here, to simplify the discussion, we assume that the achieved system reliability is *satisfactory* when there is no pre-scheduled recovery and no power management scheme is applied (i.e., all tasks are executed at f_{max}). We underline that the schemes to be studied in this paper can be applied to systems where higher levels of reliability are required as well. Without loss of generality, suppose that a recovery task RT needs to be pre-scheduled intentionally to achieve the desired high level of reliability. Consider the augmented task set $\Gamma' = \Gamma \cup \{RT\}$, from the discussion in the next two sections, applying the proposed schemes to Γ' (where the recovery task RT is treated as a *normal* task) will ensure that the reliabilities for *all* tasks in Γ' will be preserved, which will in turn preserve the required high level of system reliability.

In increasing level of sophistication and implementation complexity, we first introduce the *task-level static* RA-PM schemes and then *job-level dynamic* RA-PM schemes in the next two sections. The integration of static and dynamic schemes is further addressed in Section 6.

4 Task-Level Static RA-PM Schemes

4.1 Reliability-Aware Power Management (RA-PM)

Before presenting the proposed schemes, we first review the concept of *reliability-aware power management (RA-PM)* [38]. Instead of utilizing *all* the available slack for DVFS to save energy as in *ordinary* power management schemes which are *reliability-ignorant* (in the sense that no attention is paid to the potential effects of DVFS on task reliabilities), the central idea of RA-PM is to reserve a portion of the slack to schedule a *recovery task* (in the form of re-execution [29]) for any task whose execution is scaled down, to recuperate the reliability loss due to energy management [38].

Here, for reliability preservation, the recovery task is dispatched at the maximum frequency f_{max} only if transient fault(s) is detected at the end of the scaled task's execution. With the help of the recovery task, the overall *reliability* for a task will be the summation of the probability of the scaled task being executed correctly and the probability of having transient fault(s) during the task's scaled execution and the recovery task being executed correctly. We have shown that, **if the available slack is *more* than the WCET of a task, by scheduling a recovery task (in the form of re-execution), the RA-PM scheme can *guarantee* to preserve the reliability of a real-time job while still obtaining energy savings using the remaining slack, regardless of increased fault rates and scaled processing speeds** [38].

4.2 Task-Level RA-PM

We start with considering static RA-PM schemes that make their decisions at the *task-level*. In this approach, for simplicity, all the jobs of a task have the same treatment. That is, if a given task is selected for energy management, all its jobs will run at the same scaled frequency; otherwise, they will run at f_{max}. From the above discussion, to recuperate reliability loss due to scaled execution, each *scaled job*[2] will need a corresponding recovery job within its deadline, should a fault occur.

To provide the required recovery jobs, we construct a periodic *recovery task (RT)* by exploiting the spare CPU capacity (i.e., *static slack*). The recovery task will have the *same* timing parameters (i.e., WCET and period) as those of the task to be scaled. Therefore, with the recovery task, for each *primary* job, a recovery job can be scheduled within its deadline. Note that a recovery job is activated only when the corresponding *primary* job incurs a fault and that it is executed always at

[2]We use the expression *scaled job* to refer to any job whose execution is slowed down through DVFS, for energy management purposes.

the maximum processing speed for preserving the primary job's reliability.

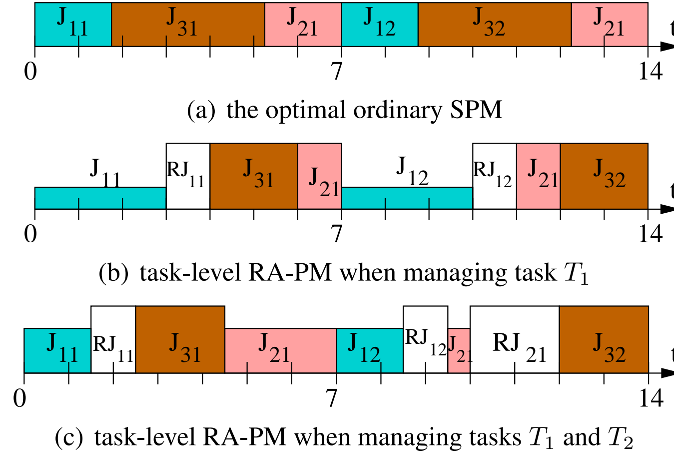

Figure 1: Static schemes for a task set with three tasks $\{T_1(1,7), T_2(2,14), T_3(2,7)\}$.

As a concrete example, suppose that we have a periodic task set of three tasks $\Gamma = \{T_1(1,7), T_2(2,14), T_3(2,7)\}$ with system utilization $U = \frac{4}{7}$. Without considering system reliability, the optimal ordinary static power management (SPM) under EDF will scale down all tasks uniformly at the speed $f = U \cdot f_{max} = \frac{4}{7}$ as shown in Figure 1(a) [4, 27]. In the figure, the X-axis represents time and the height of task boxes represents processing speed. Due to the periodicity, only the schedule within the *least common multiple (LCM)* of tasks' periods is shown. However, by uniformly scaling down the execution in this way, the reliability figures of all the tasks (and that of the system) would be significantly reduced [42].

Instead of scaling down the execution of all tasks using all the available slack, suppose that the static RA-PM scheme chooses task T_1 for management. That is, after constructing the recovery task $RT_1(1,7)$, which has the same WCET and period as those of T_1 with the utilization $ru_1 = \frac{1}{7}$, the augmented system utilization will become $U' = U + ru_1 = \frac{5}{7}$. Then, the remaining spare capacity $sc = 1 - U' = \frac{2}{7}$ will be allocated to task T_1 and all its jobs can be scaled down to the speed of $\frac{1}{3}$. With the recovery task RT_1 and the scaled execution of T_1, the *effective* system utilization is *exactly* 1 and the modified task set is schedulable under EDF as shown in Figure 1(b). From the figure, we can see that every scaled job of task T_1 has a corresponding recovery job within its deadline. Therefore, all T_1's jobs could preserve their reliability R_1^0. Since the jobs of tasks T_2 and T_3 run at f_{max}, their reliability figures are maintained at the levels of R_2^0 and R_3^0, respectively.

Therefore, by incorporating a recovery task for the task to be managed, the task-level utilization-based static RA-PM scheme could preserve system reliability while obtaining energy savings. In [39], we reported that it is not optimal (in terms of energy savings) for the RA-PM scheme to utilize

all the slack for a single task in case of *aperiodic* tasks. Similarly, we can use the spare capacity for *multiple* periodic tasks for better energy savings. For instance, Figure 1(c) shows the case where both tasks T_1 and T_2 are scaled to speed $\frac{2}{3}$ after constructing the corresponding recovery tasks RT_1 and RT_2. For illustration purposes, if we assume that the system power is given by a cubic function, simple algebra shows that managing only task T_1 could save $\frac{8}{9}E$, where E is the energy consumed by all jobs of task T_1 within LCM under no power management. In comparison, the energy savings would be $\frac{11}{9}E$ if both tasks T_1 and T_2 are managed, which is a significant improvement.

Intuitively, when more tasks are to be managed, more computation can be scaled down for more energy savings. However, more spare capacity will be reserved for recovery tasks, which, in turn, reduces the remaining spare capacity for DVFS to save energy. A natural question to ask is, for a periodic task set with multiple real-time tasks, whether there exists a fast (i.e. polynomial-time) optimal solution (in term of energy savings) for the problem of task-level utilization-based static RA-PM.

4.3 Intractability of Task-Level RA-PM

The inherent complexity of the optimal static RA-PM problem warrants an analysis. Suppose that the system utilization of the task set is U and the spare capacity is $sc = 1 - U$. If a subset Ψ of tasks are selected for management with total utilization $X = \sum_{T_i \in \Psi} u_i < sc$, after accommodating all recovery tasks, the remaining CPU spare capacity (i.e., $sc - X$) can be used to scale down the selected tasks for energy management. Considering the convex relation between power and processing speed (see Equation 1), the solution that minimizes the energy consumption will uniformly scale down all jobs of the selected tasks, where the scaled processing speed will be $f = \frac{X}{X+(sc-X)} = \frac{X}{sc}$. Since the probability of recovery jobs being activated is rather small, by ignoring the energy consumed by recovery jobs, the total energy consumption for all primary jobs (i.e., the total *fault-free* energy consumption) within LCM is found as:

$$\begin{aligned} E_{LCM} &= LCM \cdot P_s + LCM(U - X)(P_{ind} + c_{ef} \cdot f_{max}^m) \\ &\quad + LCM \cdot sc \left(P_{ind} + c_{ef} \cdot \left(\frac{X}{sc} \right)^m \right) \end{aligned} \tag{4}$$

where the first part is the energy consumption due to static power, the second part captures the energy consumption of unselected tasks, and finally, the third part represents the energy consumption of the selected tasks. Simple algebra shows that, when $X_{opt} = sc \cdot \left(\frac{P_{ind}+C_{ef}}{m \cdot C_{ef}} \right)^{\frac{1}{m-1}}$, E_{LCM} will be

minimized.

If $sc > X_{opt} \geq U$, all tasks should be scaled down appropriately to minimize energy consumption. Otherwise, the problem becomes essentially a task selection problem, where the summation of the utilization for the selected tasks should be *exactly* equal to X_{opt}, if possible. In other words, such a choice would definitely be the optimal solution. In what follows, we formally prove that the task-level utilization-based static RA-PM problem is NP-hard by transforming the PARTITION problem, which is known to be NP-hard [17], to a special case of the problem.

Theorem 1 *For a set of periodic tasks, the problem of the task-level utilization-based static RA-PM is NP-hard.*

Proof We consider a special case of the problem with $m = 2$, $C_{ef} = 1$ and $P_{ind} = 0$; that is, $X_{opt} = \frac{sc}{2}$. We show that even this special instance is intractable, by transforming the PARTITION problem, which is known to be NP-hard [17], to that special case.

In the PARTITION problem, the objective is to find whether it is possible to partition a set of n integers $a_1, \ldots, a_n$ (where $\sum_{i=1}^{n} a_i = S$) into two disjoint subsets, such that the sum of numbers in each subset is exactly $\frac{S}{2}$.

Given an instance of the PARTITION problem, we construct the corresponding static RA-PM instance as follows: we have n periodic tasks, where $c_i = a_i$ and $p_i = 2 \cdot S$. Note that, in this case, $U = \sum \frac{c_i}{p_i} = \frac{1}{2}$, $sc = 1 - U = \frac{1}{2}$. Observe that, the energy savings will be maximized if it is possible to find a subset of tasks whose total utilization is exactly $X_{opt} = \frac{sc}{2} = \frac{1}{4}$. Since $p_i = 2S \; \forall i$, this is possible if and only if one can find a subset of tasks Ψ such that $\sum_{i \in \Psi} c_i = \frac{S}{2}$. But this can happen only if the original PARTITION problem admits a YES answer. Therefore, if the static RA-PM problem had a polynomial-time solution, one could also solve the PARTITION problem in polynomial-time, by constructing the corresponding RA-PM problem, and checking if the maximum energy savings that can be obtained correspond to the amount we could gain through managing exactly $X_{opt} = \frac{sc}{2} = 25\%$ of the periodic workload.

4.4 Heuristics for Task-Level RA-PM

Considering the intractability of the problem, we propose two simple heuristics for selecting tasks for energy management: *largest-utilization-first (LUF)* and *smallest-utilization-first (SUF)*. Suppose that the tasks in a given periodic task set are indexed in the non-decreasing order of their utilizations (i.e., $u_i \leq u_j$ for $1 \leq i < j \leq n$). SUF will select the first k tasks, where k is the largest integer that

satisfies $\sum_{i=1}^{k} u_i \leq X_{opt}$. Similarly, LUF selects the task with the largest utilization first and, in the reverse order of task's utilization, tasks with smaller utilization are added to the selected subset Ψ one by one as long as $\sum_{T_k \in \Psi} u_k \leq X_{opt}$.

Here, SUF tries to manage as many tasks as possible. However, after selecting the first few tasks, if the task with the next smallest utilization can not fit into X_{opt}, SUF may be forced to use a significant portion of the spare capacity (i.e., much more than necessary) for energy management, which may not be optimal. On the contrary, LUF tries to select larger utilization tasks first, and the difference between X_{opt} and the total utilization of the selected tasks is less than the smallest utilization among all tasks. The potential drawback of LUF is that, relatively few tasks might be managed for energy savings. These heuristics are evaluated in Section 7.

5 Job-Level Dynamic RA-PM Algorithm

In our backward recovery framework, the recovery jobs are executed only if their corresponding scaled primary jobs fail. Otherwise, the CPU time reserved for recovery jobs is freed and becomes dynamic slack at run-time. Moreover, it is well-known that real-time tasks typically take a small fraction of their WCETs [16]. Therefore, significant amount of dynamic slack can be expected at run time, which should be exploited to further save energy and/or to enhance system reliability.

For ease of discussion, in this section, we first focus on the cases where no recovery task is statically scheduled. That is, for the task set with system utilization $U \leq 1$, we exploit only the dynamic slack that comes from the early completion of real-time jobs for energy and reliability management. The integrated approaches, which combine static and dynamic schemes and collectively exploit spare capacity and dynamic slack, will be discussed in Section 6.

Unlike the greedy RA-PM scheme which allocates all available dynamic slack for the next ready task when the tasks share a common deadline [38], in periodic execution settings, the run-time dynamic slack will be generated at different priorities and may not be always *reclaimable* by the next ready job [4]. Moreover, possible preemptions that a job could experience *after* it has reclaimed some slack further complicate the problem. This is because, in RA-PM framework, once a job's execution is scaled through DVFS, additional slack *must* be reserved for the potential recovery operation to preserve system reliability. *Hence, conserving the reclaimed slack until the job completes (at which point it may be used for recovery operation if faults occur, or freed otherwise) is essential in reliability-aware settings.*

5.1 Dynamic Slack Management with Wrapper-Tasks

The slack management problem for periodic tasks has been studied extensively (e.g., CASH-queue [8] and α-queue [4] approaches) for different purposes. By borrowing and also extending some fundamental ideas from these studies, we propose the *wrapper-task* mechanism to track/manage dynamic slack, which guarantees the *conservation* of the reclaimed slack, thereby maintaining the reliability figures.

Here, wrapper-tasks are used to represent dynamic slack generated at run-time. At the highest level, we can distinguish three rules for managing dynamic slack with wrapper-tasks:

- **Rule 1 (slack generation):** When new slack is generated due to *early completion of jobs* or *removal of recovery jobs*, a new wrapper-task is created with the following two timing parameters: a *size* that equals the amount of dynamic slack generated and a *deadline* that is equal to that of the job whose early completion gave rise to this slack. Then, the newly created wrapper-task will be put into a wrapper-task queue (i.e., *WT-Queue*), which is used to track/manage available dynamic slack. Here, the wrapper-tasks in *WT-Queue* are kept in the increasing order of their deadlines and all wrapper-tasks in *WT-Queue* represent slack with different deadlines. Thus, the newly created wrapper-task may be merged with an existing wrapper-task in *WT-Queue* if they have the same deadline.
- **Rule 2 (slack reclamation):** The slack is reclaimed when: **(a)** a non-scaled job has the highest priority in *Ready-Q* and its reclaimable slack is larger than the WCET of the job's task (which ensures that a recovery, in the form of re-execution, can be scheduled to preserve reliability); or, **(b)** the highest priority job in *Ready-Q* has been scaled (i.e., its recovery job has already been reserved) but its speed is still higher than f_{ee} and there is reclaimable slack. After reclamation, the corresponding wrapper-tasks are removed from *WT-Queue* and destroyed.
- **Rule 3 (slack forwarding/wasting):** After slack reclamation, the remaining wrapper-tasks in *WT-Queue* compete for CPU along with ready jobs. When a wrapper-task has the highest priority (i.e., the earliest deadline) and is "scheduled": **(a)** if there are jobs in the ready queue (*Ready-Q*), the wrapper-task will "fetch" the highest priority job in *Ready-Q* and *"wrap"* that job's execution during the interval when the wrapper-task is "executed". In this case, the corresponding slack is actually lended to the ready job and *pushed forward* (i.e. it is preserved with a later deadline); **(b)** otherwise, if there is no ready job, the CPU will become idle, and the wrapper-task is said to "execute no-ops" where the corresponding dynamic slack is consumed/wasted during this time interval. Note that, when wrapped execution is interrupted

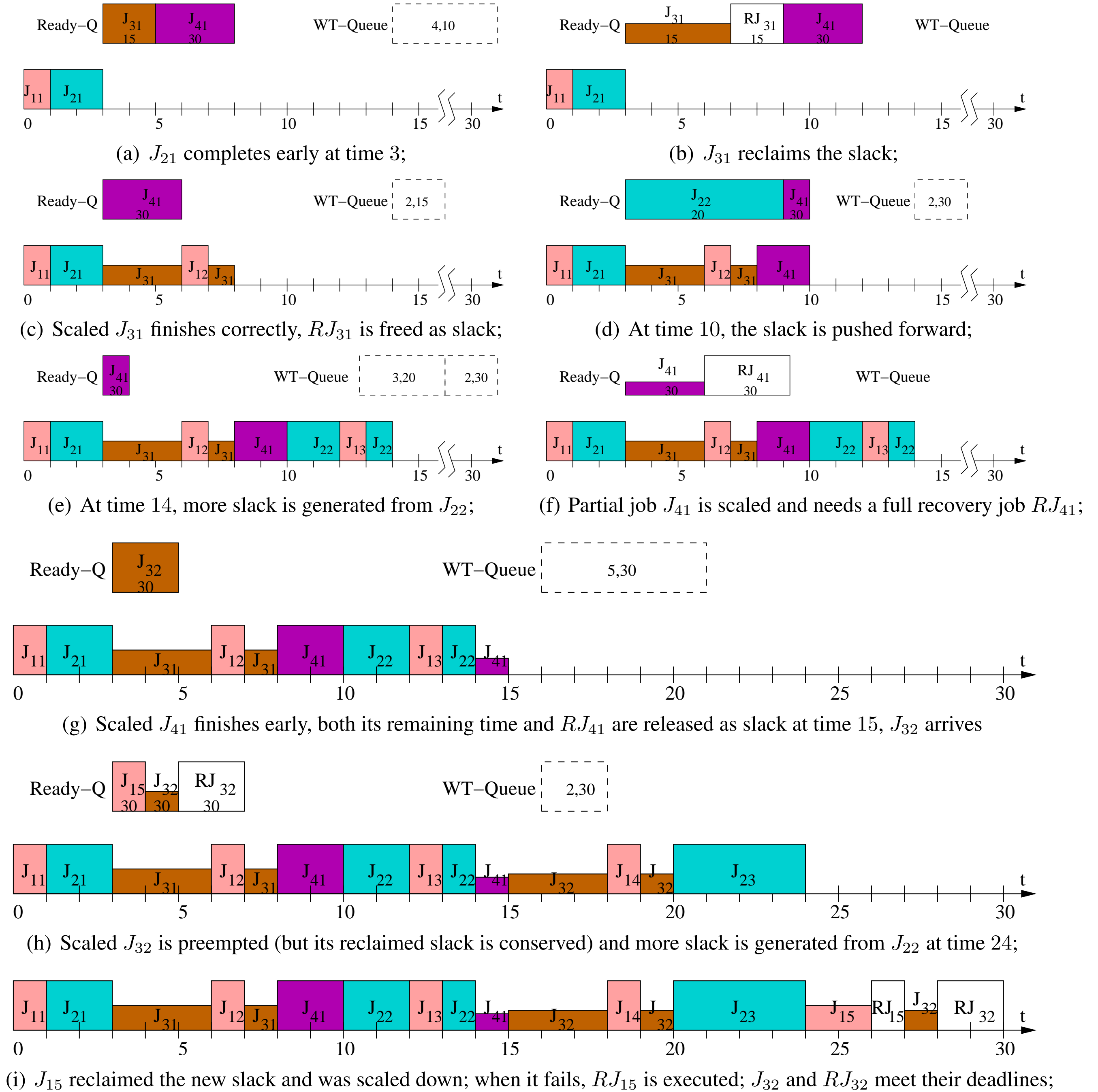

(a) J_{21} completes early at time 3;

(b) J_{31} reclaims the slack;

(c) Scaled J_{31} finishes correctly, RJ_{31} is freed as slack;

(d) At time 10, the slack is pushed forward;

(e) At time 14, more slack is generated from J_{22};

(f) Partial job J_{41} is scaled and needs a full recovery job RJ_{41};

(g) Scaled J_{41} finishes early, both its remaining time and RJ_{41} are released as slack at time 15, J_{32} arrives

(h) Scaled J_{32} is preempted (but its reclaimed slack is conserved) and more slack is generated from J_{22} at time 24;

(i) J_{15} reclaimed the new slack and was scaled down; when it fails, RJ_{15} is executed; J_{32} and RJ_{32} meet their deadlines;

Figure 2: Using wrapper-tasks to manage dynamic slack.

by higher priority jobs, only part of slack will be pushed forward (if it is consumed by the wrapped execution) or wasted, while the remaining part has the original deadline.

5.2 An Example with Wrapper-Tasks

Before formally presenting the dynamic RA-PM algorithm, in what follows, we first illustrate the idea of wrapper-tasks through a detailed example. We consider a task-set with four periodic real-time tasks $\Gamma = \{T_1(1,6),\ T_2(6,10),\ T_3(2,15),\ T_4(3,30)\}$. For jobs within time 30 (the LCM of tasks' periods), suppose that J_{21}, J_{22}, J_{23} and J_{41} take 2, 3, 4 and $2\frac{1}{3}$ time units, respectively, and all other jobs take their WCETs.

Recall that preemptive EDF scheduling is used. *For jobs with the same deadline, the one with the smaller task index is assumed to have higher priority.* When J_{21} completes early at time 3, 4 units of dynamic slack is generated and the system state is shown in Figure 2(a). Here, a wrapper-task (shown as a *dotted rectangle*) is created to represent the slack (**Rule 1**), which is labeled by two numbers: its *size* (e.g., 4) and *deadline* (e.g., 10). The job deadlines in *Ready-Q* are given by the numbers at the bottom of the job boxes.

It is known that, the slack that a job J_x can reclaim (i.e. the *reclaimable* slack) should have a deadline no later than J_x's deadline [4]. From our previous discussion, to recuperate reliability loss due to energy management, a recovery job needs to be scheduled within J_x's deadline. Hence, a non-scaled job will reclaim the slack only if the amount of reclaimable slack is larger than the job size. Thus, at time 3, J_{31} reclaims the available slack (**Rule 2a**) and scales down its execution as shown in Figure 2(b). Here, a recovery job RJ_{31} is created. The scaled execution of J_{31} uses the time slots of the reclaimed slack and is scaled at speed $\frac{2}{4} = \frac{1}{2}$, while RJ_{31} will take J_{31}'s original time slots. Both J_{31} and RJ_{31} could finish their executions within J_{31}'s deadline in the worst case scenario.

Suppose that the scaled J_{31} finishes its execution correctly at time 8, after being preempted by J_{12} at time 6. The recovery job RJ_{31} will be removed from *Ready-Q* and all its time slots will become slack (**Rule 1**) as shown in Figure 2(c). But this slack is not sufficient for reclamation by J_{41}. However, since the corresponding wrapper-task has higher priority, it is scheduled and wraps the execution of J_{41} (**Rule 3a**). When the wrapper-task finishes at time 10, a *new* wrapper-task with the same size is created, but with the deadline of J_{41}. This can also be viewed as J_{41} borrowing the slack for its execution and returning it with the extended deadline (i.e., the slack is *pushed forward*). The schedule and queues at time 10, after J_{22} arrives, are shown in Figure 2(d).

When J_{22} completes early at time 14 (after being preempted by J_{13} at time 12), 3 units of slack is generated with the deadline of 20 (**Rule 1**), as shown in Figure 2(e). Now, we have two pieces of slack (represented by two wrapper-tasks, respectively) with different deadlines.

Note that, as faults are assumed to be detected at the end of a job's execution, a *full* recovery job is needed to recuperate the reliability loss for an even *partially scaled* execution[3]. Thus, when the *partially-executed* J_{41} reclaims all the available slack (since both wrapper-tasks have deadlines no later than J_{41}'s deadline), a full recovery job RJ_{41} is created and inserted into *Ready-Q* (**Rule 2a**). J_{41} uses the remaining slack to scale down its execution appropriately as shown in Figure 2(f).

When the scaled J_{41} finishes early at time 15, both its unused CPU time and RJ_{41} are freed as slack (**Rule 1**). After the arrival of J_{32} at time 15, the schedule and queues are shown in Figure 2(g). Here, J_{32} will reclaim the slack and be scaled to speed $\frac{2}{5}$ after reserving the slack for its recovery job RJ_{32}. After the scaled J_{32} is preempted by J_{14} and J_{23} (at time 18 and 20, respectively), and J_{23} completes early at time 24, Figure 2(h) shows the newly generated slack and the state of *Ready-Q*, which contains J_{15} (with arrival time 24). Note that, the recovery job RJ_{32} (i.e., the slack time) is conserved even after J_{32} is preempted by higher priority jobs.

J_{15} reclaims the new slack. Suppose that both of the scaled jobs J_{15} and J_{32} fail, then, RJ_{15} and RJ_{32} will be executed as illustrated in Figure 2(i). It can be seen that all jobs (including recovery jobs) finish their executions on time and no deadline is missed.

5.3 Job-level Dynamic RA-PM (RA-DPM) Algorithm

The outline of the EDF-based RA-DPM algorithm is shown in Algorithm 1. Note that, RA-DPM may be invoked by three types of events: *job arrival*, *job completion* and *wrapper-task completion* (a timer can be used to signal a wrapper-task's completion to the operating systems). As common routines, we use *Enqueue(J, Q)* to add a job/wrapper-task to the corresponding queue and, *Dequeue(Q)* to fetch the highest priority (i.e., the header) job/wrapper-task and remove it from the queue. Moreover, *Header(Q)* is used to retrieve the header job/wrapper-task without removing it from the queue.

At each scheduling point, as the first step (from line 3 to line 14), the remaining execution time information of the currently running job and that of the wrapper-task (if any) is updated. If they did not complete, they are put back to *Ready-Q* and *WT-Queue* (lines 7 and 9), respectively. When a wrapper-task (WT) is used and wraps the execution of J (line 11), as discussed before, the corresponding amount of slack (i.e., t_{past}) is pushed forward by creating a new wrapper-task with the deadline of the currently wrapped job. Otherwise, the slack is consumed (wasted).

If the current job completes early (line 6) or its recovery job is removed due to the primary job's

[3] Although checkpointing could be used for partial recovery [36], we have shown that checkpoints with a single recovery section cannot guarantee to preserve task reliability [38].

Algorithm 1 EDF-based RA-DPM Algorithm

```
1: In the algorithm, t_past is the elapsed time since last scheduling point. J and WT represent the current job
   and wrapper-task, respectively (each can have the value of NULL if there is no such a job or wrapper-
   task). J.rem and WT.rem denote the remaining time requirements; J.d and WT.d are the deadlines.
2: Step 1:
3:   if (J!=NULL and J.rem − t_past > 0) {
4:     J.rem −= t_past;
5:     if (J completes) //slack of early completion
6:       Create a wrapper-task with size J.rem and deadline J.d;
7:     else Enqueue(J, Ready-Q);}
8:   if (WT!=NULL and WT.rem − t_past > 0) {
9:     WT.rem −= t_past; Enqueue(WT, WT-Queue);}
10:  if (WT!=NULL and J!=NULL) //push the slack forward;
11:    Create a wrapper-task with size t_past and deadline J.d;
12:  if (J is scaled and succeeds){
13:    RemoveRecoveryJob(J,Ready-Q);//slack from free of recovery job;
14:    Create a wrapper-task with size J.c and deadline J.d;}
15: Step 2:
16:  for (all newly arrived job NJ){ NJ.rem = NJ.c;
17:    NJ.f = f_max; Enqueue(NJ, Ready-Q);}
18: Step 3://in the following, J and WT represent the next job and wrapper-task to be processed, respec-
    tively;
19:  J=Dequeue(Ready-Q);
20:  if (J!=NULL) ReclaimSlack(J, WT-Queue);
21:  WT=Header(WT-Queue);
22:  if (J!=NULL){
23:    if (WT! = NULL and WT.d < J.d)
24:      WT = Dequeue(WT-Queue);//WT wraps J's execution
25:    else WT = NULL;//normal execution of J
26:    Execute(J);}
27:  else if (WT!=NULL)
28:    WT = Dequeue(WT-Queue);
```

successful scaled execution (lines 13 and 14), new slack is generated and corresponding wrapper-tasks are created and added to the wrapper-task queue *WT-Queue*.

Secondly, if new jobs arrive at the current scheduling point, they are added to *Ready-Q* according to their EDF priorities (line 17). The remaining timing requirements will be set as their WCETs at the speed f_{max}. The last step is to choose the next highest priority ready job J (if any) for execution (lines 19 to 28). J first tries to reclaim the available slack (line 20; details are shown in Algorithm 2). Then, depending on the priority of the remaining wrapper-tasks, J's execution may be wrapped (line 24) or executed normally (line 25). When a wrapper-task has the highest priority but no job is ready, the wrapper-task executes no-ops (line 28).

Algorithm 2 further shows the details of slack reclamation. Recall that recovery jobs are assumed

Algorithm 2 ReclaimSlack(J, *WT-Queue*)

```
1: if(J is a recovery job) return; //recovery job is not scaled
2: Step 1: //collect reclaimable slack
3:   slack = 0;
4:   for(WT ∈WT-Queue)
5:     if (WT.d ≤ J.d) slack+ = WT.rem;
6: Step 2: //scale down J if the slack is sufficient
7:   if (!J.scaled && slack <= J.c) return;//J.c is the WCET of J's task;
8:   if (!J.scaled) slack− = J.c; //reserve for recovery
9:   tmp = max(f_ee, (J.rem∗J.f)/(slack+J.rem) f_max);
10:  slack = (J.rem∗J.f)/tmp − J.rem; //slack needed for energy management
11:  J.f = tmp; //new speed
12:  if (!J.scaled){CreateRecoveryJob(J);slack+ = J.c;}
13:  J.scaled = true; //label the job as scaled
14:  //remove the reclaimed slack from WT-Queue;
15:  while (slack > 0){
16:    WT =Header(WT-Queue);
17:    if (slack ≥ WT.rem){slack− = WT.rem;
18:      WT =Dequeue(WT-Queue);}
19:    else{WT.rem− = slack; slack = 0;}
20:  }
```

to be executed at f_{max} and are not scaled (line 1). For a job J, by traversing *WT-Queue*, we can find out the amount of reclaimable slack (lines 3 and 5). If J is not a scaled job (i.e., its recovery job is not reserved yet) and the amount of reclaimable slack is no larger than the WCET of J (i.e., $J.c$), the available slack is not enough for reclamation (line 7). Otherwise, after properly reserving the slack for recovery (line 8), J's new speed is calculated, which is bounded by f_{ee} (line 9). The actual amount of slack used by J includes those for energy management (line 10) as well as the slack for recovery job (where the recovery job is created and added to *Ready-Q* in line 12). For the reclaimed slack, the corresponding wrapper-task(s) will be removed from *WT-Queue* and destroyed (lines 15 to 20), which ensures that this slack is *conserved* for the scaled job, even if higher-priority jobs preempt the scaled job's execution later.

5.4 Analysis of RA-DPM

Note that, when all jobs in a task set present their WCETs at run time, there will be no dynamic slack and no wrapper-task will be created. In this case, RA-DPM will perform the same as EDF and generate the same worst case schedule, which is feasible by assumption. However, as some jobs complete early, RA-DPM will undertake slack reclamation and/or wrapped execution, and one needs to show that the feasibility is preserved even after the changes in CPU time allocation of jobs.

Recall that, the elements of *WT-Queue* represent the slack of tasks that complete early. These slack elements, while being reclaimed, may be entirely or partially re-transformed to actual workload. Our strategy will consist in proving that, *at any time t during execution, the remaining workload could be feasibly scheduled by EDF, even if all the slack elements in WT-Queue were to be re-introduced to the system*, with their corresponding deadlines and remaining worst-case execution times (sizes). This, in turn, will allow us to show the feasibility of the actual schedule, since the above-mentioned property implies the feasibility even with an over-estimation of the actual workload, for any time t.

In RA-DPM, the slack is reclaimed for *dual* purposes of scheduling recovery jobs and slowing down the execution of tasks to save energy with DVFS. Similarly, the slack may be added to the *WT-Queue* as a result of early completion of a primary/recovery job, or de-activation of the recovery job (in case of a successful, non-faulty completion of the corresponding primary job). However, the feasibility of the resulting schedule is orthogonal to these details. Hence, we will not be further concerned about whether the slack is obtained from a primary job or a recovery job, and for what purpose (i.e. recovery or DVFS) it is used.

Before presenting the proof for the correctness of RA-DPM, we first introduce the concept of *processor demand* and the fundamental result in the feasibility analysis of periodic real-time task systems scheduled by preemptive EDF [5, 22].

Definition 1 *The* processor demand *of a real-time job set Φ in an interval $[t_1, t_2]$, denoted as $h_\Phi(t_1, t_2)$, is the sum of computation times of all jobs in Φ with arrival times greater than or equal to t_1 and deadlines less than or equal to t_2.*

Theorem 2 ([5, 22]) *A set of independent real-time jobs Φ can be scheduled (by EDF) if and only if $h_\Phi(t_1, t_2) \leq t_2 - t_1$ for all intervals $[t_1, t_2]$.*

Let us denote by $J(r, e, d)$ a job J that is released at time r, and that must complete its execution by the deadline d, with worst-case execution time e. We next prove the following lemma that will be instrumental in the rest of the proof.

Lemma 1 *Consider a set Φ_1 of real-time jobs which can be scheduled by preemptive EDF in a feasible manner. Then, the set Φ_2, obtained by replacing $J_a(r_a, e_a, d_a)$ in Φ_1 by two jobs $J_b(r_a, e_b, d_b)$ and $J_c(r_a, e_c, d_c)$, is still feasible if $e_b + e_c \leq e_a$, and $d_a \leq d_b \leq d_c$.*

Proof

Since the EDF schedule of Φ_1 is feasible, from Theorem 2, we have $h_{\Phi_1}(t_1, t_2) \leq t_2 - t_1, \forall\ t_1, t_2$. We need to show that $h_{\Phi_2}(t_1, t_2) \leq t_2 - t_1, \forall\ t_1, t_2$.

It is well-known that, when evaluating the processor demand for a set of real-time jobs, one can safely focus on intervals that start at a *job release time* and end at a *job deadline* [5, 22]. Noting that the only difference between Φ_1 and Φ_2 consists in substituting two jobs J_b and J_c for J_a, we first observe that $h_{\Phi_2}(r_x, d_y) = h_{\Phi_1}(r_x, d_y) \leq d_y - r_x$, whenever r_x is a job release time strictly greater than r_a, or d_y is a job deadline strictly smaller than d_a. Hence, we need to consider only the intervals $[r_x, d_y]$ where $r_x \leq r_a$ and $d_y \geq d_a$. By taking into account the fact that $d_a \leq d_b \leq d_c$, the following properties can be easily derived for all possible positionings of d_y with respect to these three deadlines:

- $h_{\Phi_2}(r_x, d_y) = h_{\Phi_1}(r_x, d_y) - (e_a - e_b - e_c)$ if $d_c \leq d_y$,
- $h_{\Phi_2}(r_x, d_y) = h_{\Phi_1}(r_x, d_y) - (e_a - e_b)$ if $d_a \leq d_b \leq d_y < d_c$,
- $h_{\Phi_2}(r_x, d_y) = h_{\Phi_1}(r_x, d_y) - e_a$ if $d_a \leq d_y < d_b \leq d_c$.

Since $e_a \geq e_b + e_c$ by assumption, in all three cases, $h_{\Phi_2}(r_x, d_y) \leq h_{\Phi_1}(r_x, d_y) \leq d_y - r_x$, and the job set Φ_2 is also feasible.

Now, we introduce some additional notations and definitions to reason about the execution state of RA-DPM, at time t.

- $J_R(t)$ denotes the set of ready jobs at time t. Each job $J_i \in J_R(t)$ has a corresponding remaining worst-case execution time e_i at time t and deadline d_i. Note that J_i can be seen as released at time t, and having the worst-case execution time e_i and deadline d_i.
- $J_F(t)$ denotes the set of jobs that will arrive *after* t, with their corresponding worst-case remaining execution times and deadlines.
- $J_W(t)$ denotes the set of jobs obtained through the *WT-Queue*. Specifically, for every slack element in *WT-Queue* with size s_i and deadline d_i, $J_W(t)$ will include a job $J_i(t, s_i, d_i)$.

Definition 2 *The* Augmented Remaining Workload *of RA-DPM at time* t*, denoted by* ARW(t)*, is defined as* $J_R(t) \bigcup J_F(t) \bigcup J_W(t)$.

Informally, *ARW(t)* denotes the total workload obtained, if one re-introduces *all* the slack elements in *WT-Queue* at time t to the ready-queue, with their corresponding deadlines. This is clearly an

over-estimation of the actual workload at time t, since the amount of workload re-introduced by slack reclamation can never exceed $J_W(t)$.

Theorem 3 ARW(t) *can be scheduled by EDF in a feasible manner during the execution of RA-DPM, for every time t.*

Proof The statement is certainly true at $t = 0$, when the *WT-Queue* is empty, and the workload can be scheduled in a feasible manner by EDF even under the worst-case conditions.

Assume that the statement holds $\forall t \leq t_1$. Note that for $t = t_1, t_1 + 1, \ldots,$ *ARW(t)* remains feasible as long as there is no slack reclamation or 'wrapped execution'. This is because, under these conditions, the task with highest priority in the ready queue is executed at every time slot according to EDF – and being an optimal preemptive scheduling policy, EDF preserves the feasibility of the remaining workload. Also note that, if the ready queue is empty for a given time slot, then the slack at the head of *WT-Queue* is consumed, which corresponds to the fact that *ARW(t)* is updated dynamically according to EDF execution rules.

Let t_2 be the first time instant after t_1, if any, where RA-DPM performs a slack reclamation or starts the "wrapped execution". We denote the head of *WT-Queue* by H at $t = t_2$, with deadline d_H and size e_H. We will show that *ARW()* remains feasible after such a point in both scenarios, completing the proof.

- **Case 1:** At $t = t_2$, slack reclamation is performed through the *WT-Queue*. Assume k units of slack is transferred from H to the job J_A which is about to be dispatched, with deadline $d_A \geq d_H$ and remaining worst-case execution time e_A. Note that this slack transfer can be seen as replacing $J_H(t_2, e_H, d_H)$ in *ARW(t_2)* by two new jobs $J_{H_1}(t_2, k, d_A)$ and $J_{H_2}(t_2, e_H - k, d_H)$; and by the virtue of Lemma 1, *ARW(t_2)* remains feasible after the slack transfer. If, the slack is transferred from multiple elements in *WT-Queue* successively, then we can repeat the argument for the following elements in the same order.

- **Case 2:** At $t = t_2$, a 'wrapped execution' starts, to end at $t = t_3 > t_2$. We will show that *ARW(t)* remains feasible for $t_2 \leq t \leq t_3$, completing the proof.

  The wrapped execution (i.e., slack forwarding) in the interval $[t_2, t_3]$ is functionally equivalent to the following: in every time slot $[t_i, t_{i+1}]$ in the interval $[t_2, t_3]$, one unit of slack from H (the head of *WT-Queue*) is replaced by another item in *WT-Queue* with size 1, and deadline d_{A_i}, which is the deadline of job J_{A_i} that executes on the CPU in the interval $[t_i, t_{i+1}]$. On

the other hand, when seen from the perspective of changes in *ARW(t)*, this is equivalent to the reclamation by J_{A_i} one unit of slack from H in slot $[t_i, t_{i+1}]$ (even though, in actual execution, this slack unit will not be used because of wrapped execution). As a conclusion, *ARW(t)* remains feasible at every time slot in the interval $[t_2, t_3]$ as slack reclamation on *ARW(t)* was shown to be safe in Case 1 above.

Since *ARW(t)* is an over-estimation of the actual workload, we obtain the following result:

Corollary 1 *RA-DPM preserves the feasibility of any periodic real-time task set under preemptive EDF.*

5.5 Complexity of RA-DPM

Note that, in the worst case (e.g., at $t = 0$), n jobs can arrive simultaneously, and the complexity of building *Ready-Q* (lines 16 and 17 of Algorithm 1) will be $O(n \cdot log(n))$. Moreover, the deadlines of wrapper-tasks are actually the deadlines of corresponding real-time jobs. At any time t, there are at most n different deadlines corresponding to jobs with release times on or before t *and* deadlines on or after t. That is, the number of wrapper-tasks in ***WT-Queue*** is at most n. Therefore, slack reclamation, where multiple wrapper-tasks may be reclaimed at the same time, can be performed (by traversing *WT-Queue*; see Algorithm 2) in time $O(n)$. Hence, the complexity of RA-DPM is at most $O(n \cdot log(n))$ at each scheduling point.

6 Integrated Schemes

We have studied separately, in the last two sections, the task-level static and job-level dynamic RA-PM schemes that exploit system spare capacity (i.e., *static slack*) and dynamic slack, respectively. In what follows, depending on how the static and dynamic slack are collectively reclaimed, we will present two different approaches that integrate the static and dynamic schemes in reliability-aware settings.

6.1 RA-DPM over Static Schemes

The intuitive approach, which follows the same idea of applying dynamic slack reclamation on top of static power management [4], is to apply RA-DPM to a task set that has been statically managed. In this case, a subset of tasks are statically selected to scale down and each of them has a corresponding

recovery task for reliability preservation utilizing the spare capacity, which is different from the original task set (where all tasks run at the maximum frequency and no spare capacity is reclaimed). Therefore, for jobs of different tasks, RA-DPM needs to treat them differently at the time of their arrivals (i.e., at lines 16 and 17 of Algorithm 1).

Specifically, for jobs of tasks that are not scaled down, they will be handled in the same way as shown in Algorithm 1. However, for jobs of scaled tasks, their initial speed will not be f_{max} but a pre-determined scaled speed (e.g., $NJ.f = f < f_{max}$). The worst case remaining execution time and flags should be set accordingly (e.g., $NJ.rem = \frac{NJ.c}{f}$; $NJ.scaled = true$;) and corresponding recovery jobs should be created. After that, these pre-scaled jobs can be treated the same as jobs that are scaled online. That is, if their scaled speed is higher than f_{ee}, they may reclaim additional dynamic slack and further slow down their executions. When they complete successfully, the corresponding recovery jobs will be removed/released and become dynamic slack; otherwise, the recovery jobs will be activated accordingly.

Note that, after a feasible task set (with system utilization $U \leq 1$) is managed statically, the *effective* total system utilization of the augmented task set (with scaled tasks and newly constructed recovery tasks) should still be less than or equal to 1 (see Section 4). That is, the augmented task set is schedulable under preemptive EDF. From previous discussion, we know that RA-DPM does not introduce any additional workload to the augmented task set. Therefore, the approach of applying RA-DPM over static RA-PM schemes is feasible in terms of meeting all the deadlines.

6.2 Slack Transformation using A Dummy Task

In the previous approach, spare capacity (i.e., static slack) and dynamic slack are reclaimed in two separate steps. To simplify the process, in this section, we consider a single-step approach where the spare capacity will be *transformed* into dynamic slack and is reclaimed at run time. The central idea of such slack transformation relies on the creation of a *dummy task* T_0 using the spare capacity. That is, the utilization of T_0 is $u_0 = sc = 1 - U$. At run time, all jobs of the dummy task will have the *zero* actual execution time, which effectively transforms the spare capacity to dynamic slack periodically. Therefore, with this approach, all available slack can be managed/reclaimed by the dynamic scheme (i.e., RA-DPM) *uniformly*. In this approach, since a separate static component does not exist, at system start time, all jobs will assume (implicitly) the speed f_{max}. However, at dispatch time, many jobs will be able to slow down thanks to the dynamic slack periodically introduced by the dummy task T_0.

Note that, regardless of the period of T_0, the task set augmented with the dummy task is schedulable under preemptive EDF. Therefore, it is also schedulable under RA-DPM. However, we can see that the period of the dummy task will lead to an interesting trade-off between the slack usage efficiency and the overhead of RA-DPM. Intuitively, for smaller periods, the dummy task will distribute the slack across the schedule more evenly and thus increase the chance of the slack being reclaimed. However, with smaller periods, more preemptions, and scheduling points/activities can be expected (thus resulting in higher scheduling overhead). Conversely, larger periods for the dummy task will incur less scheduling overhead, but the chance of the corresponding slack being reclaimed will be reduced and the slack is more likely to be wasted. The effects of the dummy task's period on the performance and overhead of RA-DPM will be evaluated in the next section.

7 Simulation Results and Discussion

To evaluate the performance of our proposed schemes, we developed a discrete event simulator using C++. In the simulations, we consider the following different schemes. The scheme of *no power management (NPM)*, which executes all tasks/jobs at f_{max} and puts system to sleep states when idle, is used as the baseline for comparison. The *ordinary static power management (SPM)* scales all tasks uniformly at speed $f = U \cdot f_{max}$ (where U is the system utilization). For the task-level static RA-PM schemes, after obtaining the optimal utilization (X_{opt}) that should be managed, two heuristics are considered: *smaller utilization task first (RA-SPM-SUF)* and *larger utilization task first (RA-SPM-LUF)*. For dynamic schemes, we implemented our *job-level dynamic RA-PM (RA-DPM)* algorithm and the *cycle conserving EDF (CC-EDF)* [27], a well-known but reliability-ignorant DVFS algorithm, for periodic real-time tasks.

Transient faults are assumed to follow the Poisson distribution with an average fault rate of $\lambda_0 = 10^{-6}$ at f_{max} (and corresponding supply voltage), which corresponds to 100,000 FITs (failures in time, in terms of errors per billion hours of use) per megabit. This is a realistic fault rate as reported in [18, 46]. To take the effects of DVFS on fault rates into consideration, we adopt the exponential fault rate model developed in [42], where $\lambda(f) = \lambda_0 \cdot g(f) = \lambda_0 10^{\frac{d(1-f)}{1-f_{min}}}$. Here, the exponent d (> 0) is a constant which indicates the sensitivity of fault rates to DVFS. The maximum fault rate is assumed to be $\lambda_{max} = \lambda_0 10^d$, which corresponds to the minimum frequency f_{ee} (and corresponding supply voltage). In our simulations, we assume that the exponent $d = 2$. That is, the average fault rate is assumed to be 100 times higher at the lowest speed f_{min} (and corresponding supply voltage). The effects of different values of d were evaluated in our previous work [38, 39, 42].

As discussed in Section 3, the static power P_s will be always consumed for all schemes. Therefore, we focus on active power in our evaluations. We further assume that $m = 3$, $C_{ef} = 1$ and $P_{ind} = 0.1$. In these settings, the energy efficient frequency is found as $f_{ee} = 0.37$ (see Section 3). The effects of these parameters on normalized energy consumption have been studied extensively in our previous work [43].

We consider synthetic real-time task sets where each task set contains 5 or 20 periodic tasks. The periods of tasks (p) are uniformly distributed within the range of $[10, 20]$ (for short-period tasks) or $[20, 200]$ (for long-period tasks). The WCETs of tasks are uniformly distributed in the range of 1 and their periods. Finally, the WCETs of tasks are scaled by a constant such that the system utilization of tasks reaches a desired value [27]. The variability in the actual workload is controlled by the $\frac{WCET}{BCET}$ ratio (that is, the worst-case to best-case execution time ratio), where the actual execution time of tasks follows a normal distribution with mean and standard deviation being $\frac{WCET+BCET}{2}$ and $\frac{WCET-BCET}{6}$, respectively [4].

We simulate the execution for 10^7 and 10^8 time units, for short- and long-period task sets, respectively. That is, approximately 5 to 20 million jobs are executed during each run. Moreover, for each result point in the graphs, 100 task sets are generated and the presented results correspond to the average.

7.1 Performance of Task-Level Schemes

For different system utilization (i.e., spare capacity), we first evaluate the performance of the task-level static schemes. It is assumed that all jobs take their WCETs. For task sets with short periods (i.e., $p \in [10, 20]$), where each set contains 20 tasks, Figure 3a first shows the probability of failure (i.e., $1-$*reliability*) for NPM and the static schemes. Here, the probability of failure shown is the ratio of the number of failed jobs (recovery jobs have been incorporated, if any) over the total number of jobs executed.

From the figure, we can see that, as the system utilization increases, for NPM, the probability of failure increases slightly. The reason for this is that, with increased total utilization, the computation requirement for each task increases and tasks run longer, which increases the probability of being subject to transient fault(s). The probability of failure for SPM increases drastically due to increased fault rates and extended execution time. Note that, the minimum energy efficient frequency is $f_{ee} = 0.37$. At low system utilizations (i.e., $U < 0.37$), SPM executes all tasks with f_{ee}. The probability of failure for SPM increases slightly with increased utilization for the same reason as

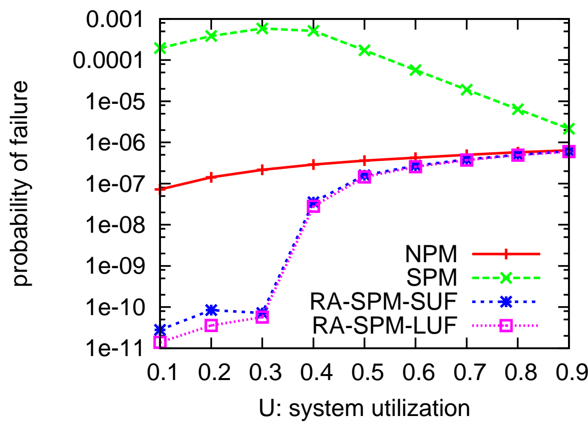

(a) 20 tasks with $p \in [10, 20]$

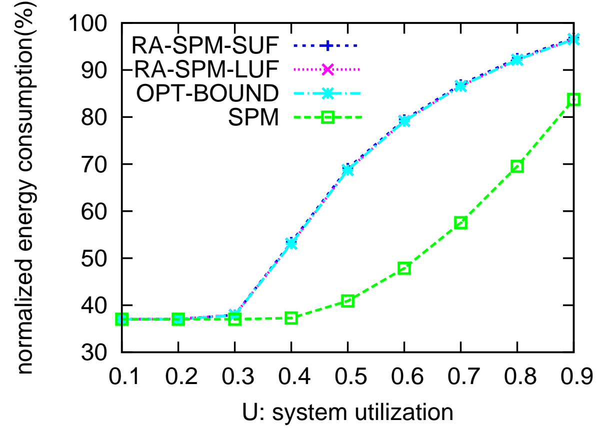

(b) 20 tasks with $p \in [10, 20]$

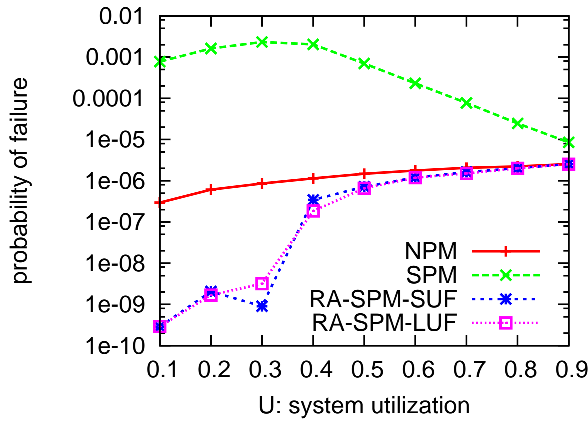

(c) 5 tasks with $p \in [10, 20]$

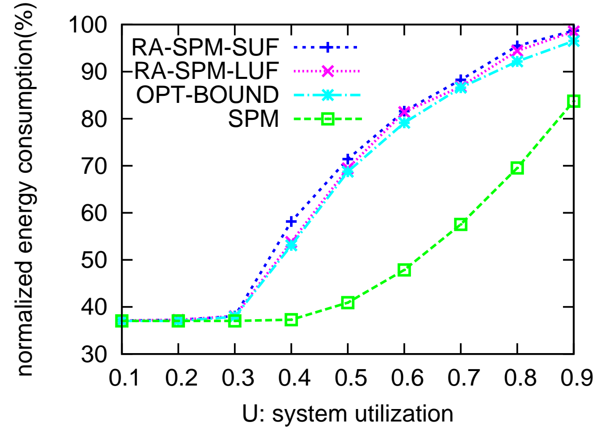

(d) 5 tasks with $p \in [10, 20]$

Figure 3: Reliability and energy consumption for static schemes.

NPM. However, when the system utilization is higher than 0.37, the processing speed of SPM increases with increased utilization, which has lower failure rates and results in decreased probability of failure.

For reliability-aware static schemes (i.e., RA-SPM-SUF and RA-SPM-LUF), by incorporating a recovery task for each task to be scaled, the probability of failure is lower than that of NPM and system reliability is preserved, which confirms the theoretical result obtained in Section 4.

Figure 3b further shows the normalized energy consumption for tasks under different schemes with NPM as a baseline. Here, reliability-aware static schemes consume up to 30% more energy than that of the ordinary SPM because there is less spare capacity available for energy management. Moreover, the figure also shows the energy consumption for *OPT-BOUND*, which is calculated as the fault-free energy consumption with the assumption that the managed tasks have the accumulated utilization *exactly* equal to X_{opt} (See Section 4.3). Clearly, *OPT-BOUND* provides an upper-bound

even for the *optimal* static solution. From the figure, we can see that the normalized energy consumption for the two heuristics is almost the same as that of the upper bound (within 2%). With 20 tasks in a task set, each task has a very small utilization, which leads to the close-to-optimal solution for both static heuristics.

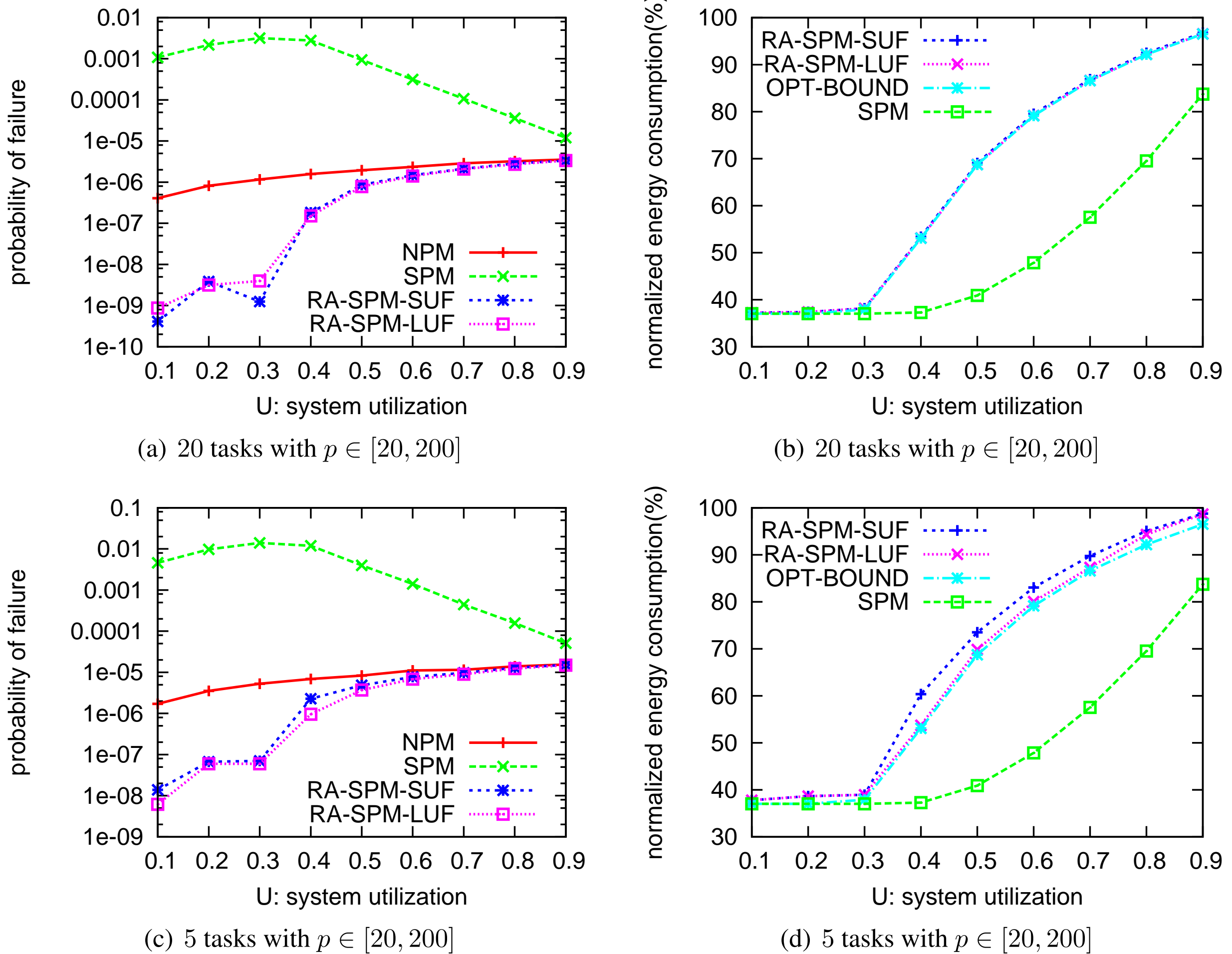

(a) 20 tasks with $p \in [20, 200]$

(b) 20 tasks with $p \in [20, 200]$

(c) 5 tasks with $p \in [20, 200]$

(d) 5 tasks with $p \in [20, 200]$

Figure 4: Reliability and energy consumption for static schemes.

When there are only 5 tasks in a task set, the utilization for each task becomes larger and Figure 3d shows the normalized energy consumption for the static heuristics and the upper-bound. From the results, we can see that RA-SPM-LUF outperforms RA-SPM-SUF for most cases since it selects tasks to more closely match X_{opt}. However, even for RA-SPM-SUF, the normalized energy consumption is within 5% of that of the upper-bound. For long-period tasks (i.e., $p \in [20, 200]$), similar results are obtained and are shown in Figure 4.

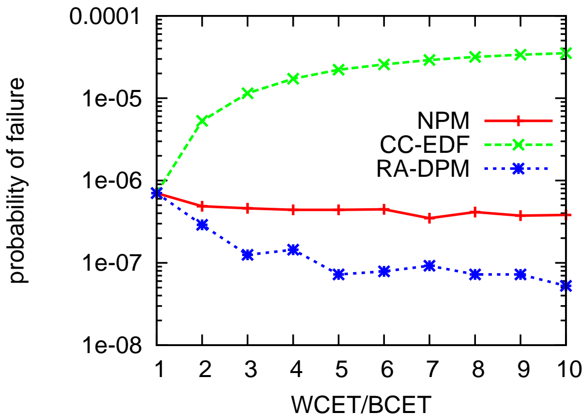

a. reliability for $p \in [10, 20]$

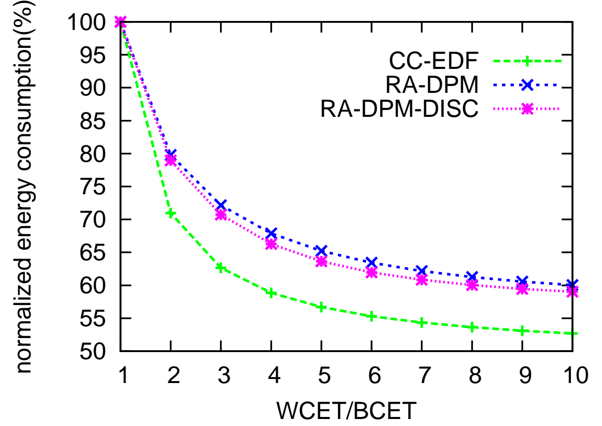

b. energy for $p \in [10, 20]$

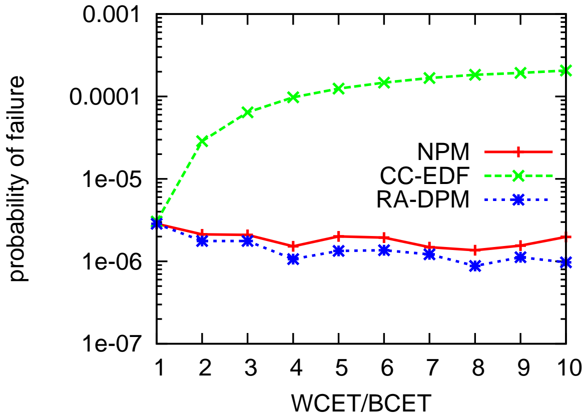

c. reliability for $p \in [20, 200]$

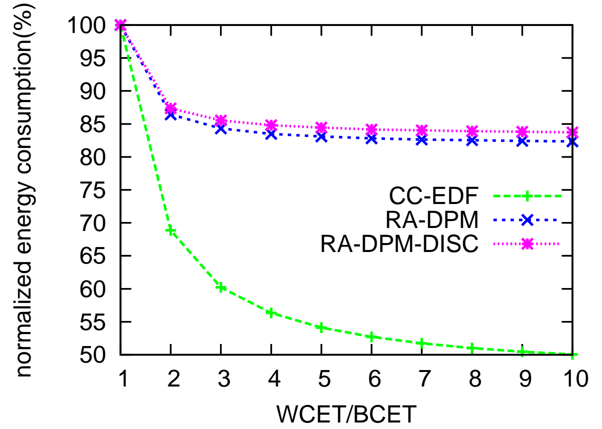

d. energy for $p \in [20, 200]$

Figure 5: Reliability and energy consumption for dynamic schemes with 20 tasks.

7.2 Performance of Job-Level Schemes

With system utilization fixed at $U = 1.0$ (i.e., no static slack is available), we vary $\frac{WCET}{BCET}$ ratio and evaluate the performance of the dynamic schemes. Figure 5a first shows the probability of failure for short-period tasks (i.e., $p \in [10, 20]$) with each task set contains 20 tasks. Here, as $\frac{WCET}{BCET}$ ratio increases, more dynamic slack becomes available. Without considering system reliability, CC-EDF uses all available slack greedily for energy savings and its probability of failure increases (i.e., system reliability decreases) drastically due to the scaled executions of jobs. Again, by reserving slack for recovery jobs before using it for saving energy, RA-DPM preserves system reliability. When there is more dynamic slack as the value of $\frac{WCET}{BCET}$ increases, more recovery jobs will be scheduled and, compared to that of NPM, the probability of failure for RA-DPM generally decreases (i.e., better system reliability is achieved).

Figure 5b shows the normalized energy consumption for short-period tasks. Initially, as the ratio of $\frac{WCET}{BCET}$ increases, additional dynamic slack becomes available and normalized energy consumption decreases. Due to the limitation of f_{ee} ($= 0.37$), when $\frac{WCET}{BCET} > 9$, the normalized energy consumption for both schemes stays roughly the same and RA-DPM consumes about 8% more energy than CC-EDF. However, for long-period tasks (i.e., $p \in [20, 200]$), as shown in Figure 5cd, RA-DPM performs much worse than CC-EDF and consumes about 32% more energy. A possible explanation is that, when the slack is pushed forward excessively by the long-period tasks, this prevents other jobs from reclaiming it (due to reduced slack priorities), resulting in less energy savings. Similar results are obtained for cases where each task set contains 5 tasks.

7.3 Effects of Discrete Speeds

So far, we have assumed that the clock frequency can be scaled continuously. However, current DVFS-enabled processors (e.g., Intel XScale [1, 2]) only have a few speed levels. Nevertheless, our schemes can be easily adapted to discrete speed settings. After obtaining the desired speed (e.g., Algorithm 2 line 9), we can either use two adjacent frequency levels to emulate the task's execution at that speed [20], or use the next higher discrete speed to ensure the algorithm's feasibility. Assuming Intel XScale model [1] with 5 speed levels $\{0.15, 0.4, 0.6, 0.8, 1.0\}$ and using the next higher speed, we re-ran the simulations. The results for normalized energy consumption are represented as *RA-DPM-DISC* and shown in Figure 5bd. Here, we can see that, although RA-DPM-DISC consumes slightly less energy than that of RA-DPM for short period tasks; for long-period tasks, RA-DPM performs slightly better than RA-DPM-DISC. However, the difference on the energy consumption for discrete speeds and continuous speed is within 2%. The reason is that, with the next higher discrete speed being utilized, the unused slack is not wasted but actually saved for future usage.

7.4 Evaluation of the Integrated Schemes

In the evaluation of the integrated schemes, we consider three different algorithms for comparison. First, the static RA-SPM-SUF scheme, which executes selected tasks at statically determined scaled frequency but does not reclaim dynamic slack at run time. *SUF+RA-DPM* is the second scheme that will reclaim dynamic slack to further scale down the statically selected tasks or to manage more unscaled tasks at run time. The last scheme, *DUMMY+RA-DPM*, uses a dummy task (as discussed in Section 6) and does not select any task for scaling down statically. At run-time, together with the transformed dynamic slack from the dummy task, all dynamic slack will be reclaimed appropriately

as in RA-DPM.

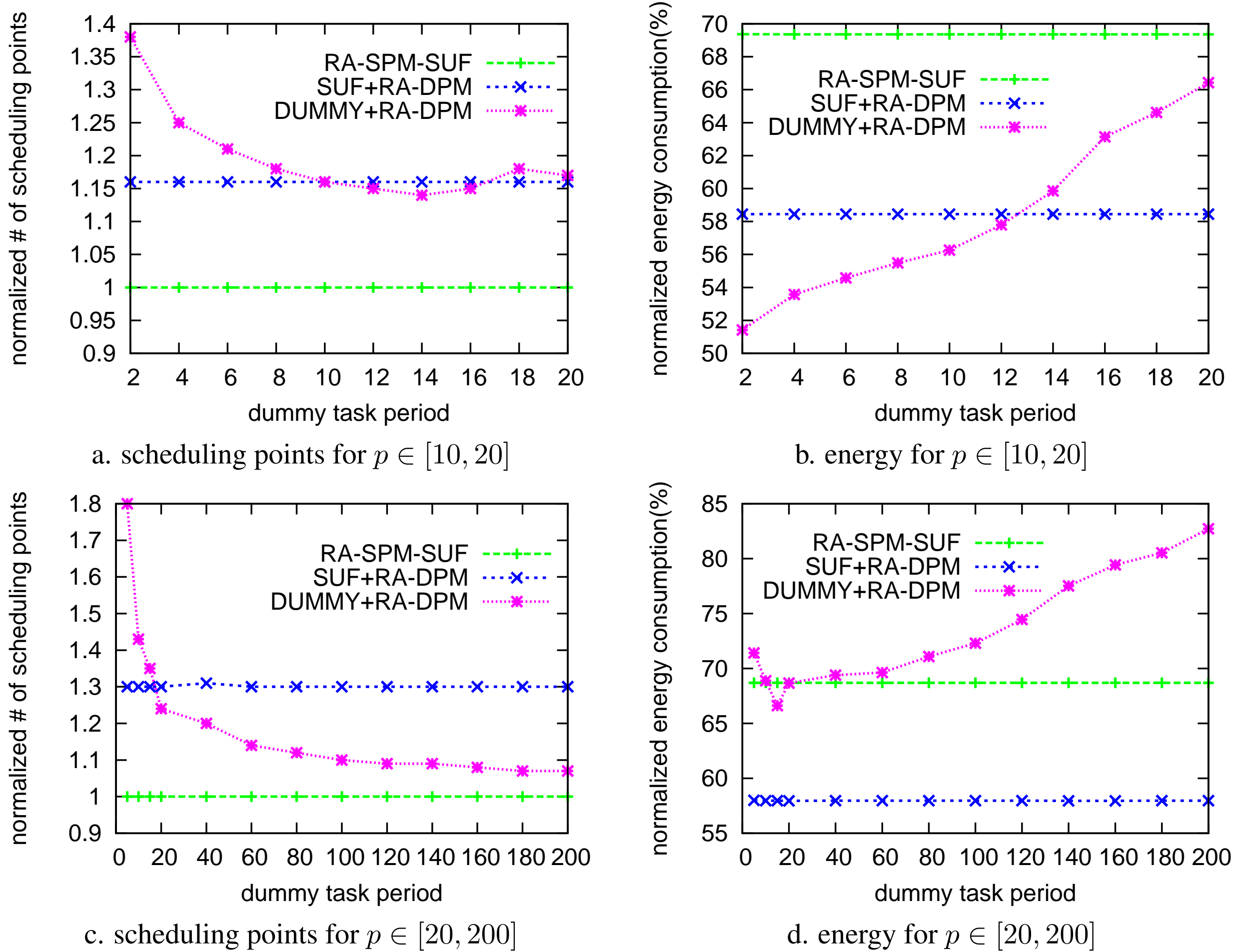

Figure 6: Effects of the dummy task's period. Here, $U = 0.5$ and $\frac{WCET}{BCET} = 1$.

For task sets with 20 short-period tasks (i.e., $p \in [10, 20]$) with system utilization $U = 0.5$ and $\frac{WCET}{BCET} = 1$, Figure 6a first shows the normalized number of scheduling points with NPM as the baseline for different periods of the dummy task. Note that, the dummy task only affects DUMMY+RA-DPM scheme and the number of scheduling points for RA-SPM-SUF and SPM+RA-DPM remain the same for different dummy task periods. Without managing and reclaiming the dynamic slack (from early completion of jobs and the removal of statically scheduled recovery jobs), the number of scheduling points for RA-SPM-SUF is almost the same as that of NPM. For SUF+RA-DPM, it reclaims dynamic slack at run-time and the number of scheduling points is about 16% more than that of NPM. For DUMMY+RA-DPM, as the period of the dummy task increases, less scheduling activities are expected and the normalized number of scheduling points decreases.

From the figure, we can see that, the minimum number of scheduling points is obtained when the dummy period is 14 (which is around 10, the smallest period of tasks in the task set). For larger dummy task periods, the transformed slack is aggregated and the job that reclaims the slack is more likely executed at the minimum frequency f_{ee}, which leads to more preemption and thus more scheduling points.

Figure 6b further shows the corresponding normalized energy consumption for the three schemes. By reclaiming the dynamic slack, SUF+RA-DPM could save roughly 12% more energy than that of RA-SPM-SUF. When the period of the dummy task is less than 10, the transformed slack is uniformly distributed and can be effectively reclaimed, which leads to better energy savings for DUMMY+RA-DPM than that of SUF+RA-DPM. However, for larger dummy task periods, the transformed slack is aggregated under DUMMY+RA-DPM and leads to uneven execution for tasks, where more energy is consumed under DUMMY+RA-DPM than that of SUF+RA-DPM. From these results, we can see that, for short period tasks, *the best period for the dummy task would be the minimum period of all tasks in a task set*, which is further confirmed for long-period tasks as shown in Figure 6cd. However, for long-period tasks, the energy consumption for DUMMY+RA-DPM is much worse than that of SUF+RA-DPM. This is because, the transformed dynamic slack under DUMMY+RA-DPM may be pushed forward too much and wasted, which leads to inefficient usage of the static slack and more energy consumption compared to that of SUF+RA-DPM.

For different values of $\frac{WCET}{BCET}$ (i.e., different amounts of dynamic slack), Figure 7 further shows the performance of the integrated schemes with 20 tasks in the task sets. For short-period (i.e., $p \in [10, 20]$) tasks with system utilization $U = 0.5$, Figures 7ab first show the probability of failure and normalized energy consumption for all the schemes, respectively. The same as before, all reliability-aware schemes perform better than NPM with lower probability of failure. By reclaiming dynamic slack and managing more jobs at run time, SUF+RA-DPM achieves better system reliability (i.e., lower probability of failure values) than that of RA-SPM-SUF. With the dummy task's period being set as 10, DUMMY+RA-DPM performs slightly better (in terms of both reliability and energy) than SUF+RA-DPM when $\frac{WCET}{BCET} = 1$. That is, when there is no dynamic slack available from early completion (i.e., $\frac{WCET}{BCET} = 1$), by using a dummy task to transform *all* spare capacity to dynamic slack, DUMMY+RA-DPM can use it more effectively to scale down the jobs to f_{ee} for more energy savings and possibly re-use such slack to manage more jobs for better system reliability. However, for cases where dynamic slack from early completion is significant (i.e., $\frac{WCET}{BCET} >= 2$), DUMMY+RA-DPM could be too greedy when using the dynamic slack and the slack transformed from spare capacity by the dummy task, and thus performs slightly worse ($\leq 3\%$)

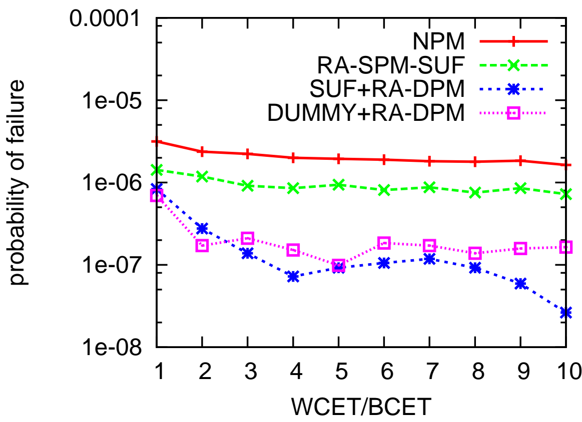

a. reliability for $U = 0.5$ and $p \in [10, 20]$

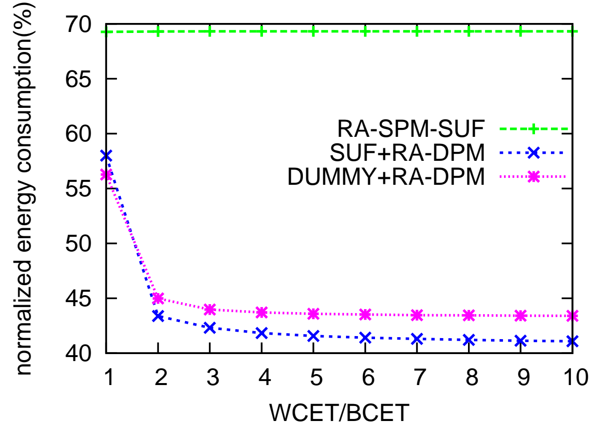

b. energy for $U = 0.5$ and $p \in [10, 20]$

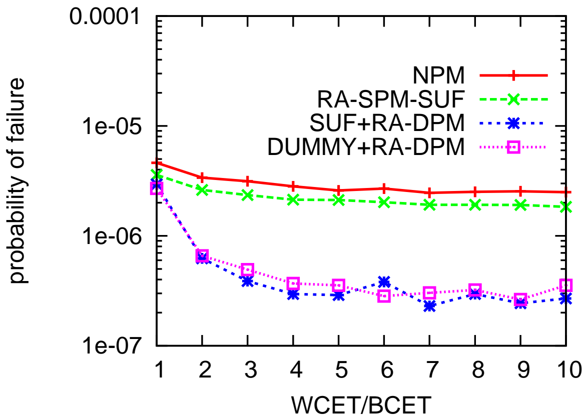

c. reliability for $U = 0.7$ and $p \in [10, 20]$

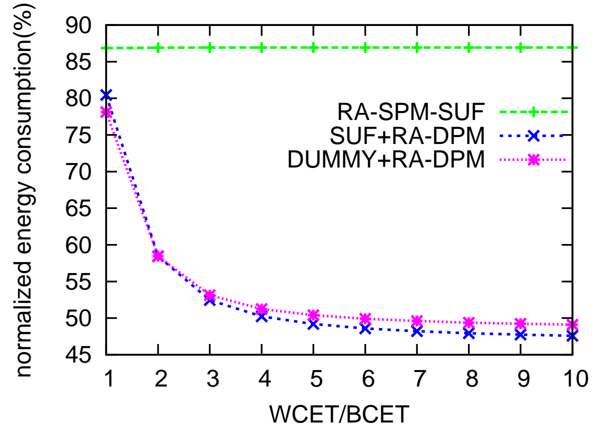

d. energy for $U = 0.7$ and $p \in [10, 20]$

Figure 7: Performance of the integrated schemes with 20 tasks.

than SUF+RA-DPM. For task sets with higher system utilization $U = 0.7$, similar results are shown in Figure 7cd, where the performance difference between SUF+RA-DPM and DUMMY+RA-DPM becomes smaller. For long-period (i.e., $p \in [20, 200]$) tasks, a larger performance difference between SUF+RA-DPM and DUMMY+RA-DPM has been observed and the results are shown in Figure 8.

8 Conclusions and Future Work

DVFS was recently shown to have negative impact on settings where transient faults become more prominent with continued scaling of CMOS technologies and reduced design margins. In this paper, focusing on preemptive EDF scheduling, we proposed a reliability-aware power management (RA-PM) framework for *periodic* real-time tasks. We first studied *task-level* utilization-based static

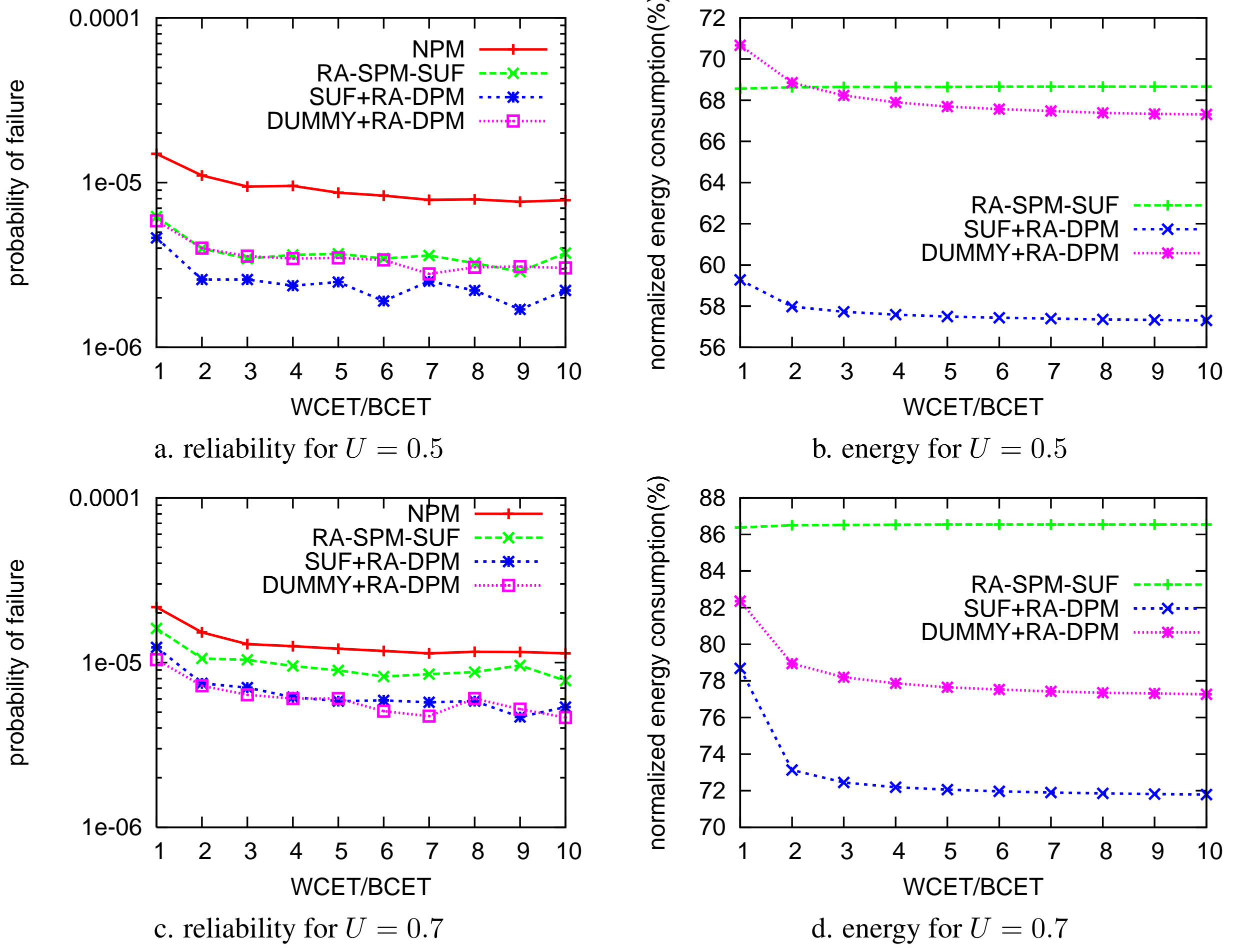

Figure 8: Performance of the integrated schemes with 20 tasks and $p \in [20, 200]$.

RA-PM schemes that exploit the system spare capacity. We showed the *intractability* of the problem and proposed two efficient heuristics. Moreover, we proposed the *wrapper-task* mechanism for efficiently managing dynamic slack and presented a *job-level* dynamic RA-PM scheme. The scheme is able to *conserve* the slack reclaimed by a scaled job, which is an essential requirement for reliability preservation, across preemption points. The correctness of the dynamic scheme in terms of meeting all the timing constraints is formally proved. In addition, two integrated techniques that combine the management of static and dynamic slack are also studied. The first technique applies job-level dynamic scheme to a statically managed task set. In the second technique, the spare capacity is used to create a dummy task and the job-level dynamic scheme is applied to the augmented task set, where the spare capacity will be transformed to dynamic slack by the dummy task at run-time.

The proposed schemes are evaluated through extensive simulations with synthetic real-time work-

loads. The results show that, compared to the ordinary energy management schemes, the new schemes could achieve comparable amount of energy savings while preserving system reliability. However, ordinary energy management schemes that are *reliability-ignorant*, often lead to drastically decreased system reliability. For the static heuristics, the energy savings are close to the upper-bound of the optimal solution by a margin of 5%. By effectively exploiting the run-time slack, additional energy savings can be obtained through the dynamic schemes while preserving system reliability. For the integrated technique with a dummy task, the period of the dummy task should be set as the minimum period of tasks in a task set for the best performance. Although the dummy task approach simplifies the slack reclamation, applying job-level dynamic scheme on top of task-level static scheme generally gives better performance.

As our future work, we plan to extend the RA-PM framework for sporadic real-time tasks as well as mixed workload with both aperiodic and periodic tasks. Another direction will be extending the current RA-PM framework to consider parallel multicore-based systems and various system reliability requirements.

References

[1] Intel xscale technology and processors. http://developer.intel.com/design/intelxscale/.

[2] Intel corp. mobile pentium iii processor-m datasheet. Order Number: 298340-002, Oct 2001.

[3] H. Aydin, V. Devadas, and D. Zhu. System-level energy management for periodic real-time tasks. In *Proc. of The* 27th *IEEE Real-Time Systems Symposium (RTSS)*, Piscataway, NJ, USA, Dec. 2006. IEEE CS Press.

[4] H. Aydin, R. Melhem, D. Mossé, and P. Mejia-Alvarez. Power-aware scheduling for periodic real-time tasks. *IEEE Trans. on Computers*, 53(5):584–600, 2004.

[5] S. Baruah, R. Howell, and L. Rosier. Algorithms and complexity concerning the preemptive scheduling of periodic, real-time tasks on one processor. *Real-Time Systems*, 2, 1990.

[6] E. Bini, G.C. Buttazzo, and G. Lipari. Speed modulation in energy-aware real-time systems. In *Proc. of the* 17th *Euromicro Conference on Real-Time Systems*, 2005.

[7] T. D. Burd and R. W. Brodersen. Energy efficient cmos microprocessor design. In *Proc. of The HICSS Conference*, Jan. 1995.

[8] M. Caccamo, G. Buttazzo, and L. Sha. Capacity sharing for overrun control. In *Proc. of Real-Time Systems Symposium*, 2000.

[9] X. Castillo, S. McConnel, and D. Siewiorek. Derivation and caliberation of a transient error reliability model. *IEEE Trans. on computers*, 31(7):658–671, 1982.

[10] J.-J. Chen and T.-W. Kuo. Multiprocessor energy-efficient scheduling for real-time tasks with different power characteristics. In *Proc. of the 2005 International Conference on Parallel Processing (ICPP)*, pages 13–20, Jun. 2005.

[11] J.-J. Chen and T.-W. Kuo. Procrastination determination for periodic real-time tasks in leakage-aware dynamic voltage scaling systems. In *Proc. of the 2007 IEEE/ACM Int'l Conference on Computer-Aided Design (ICCAD)*, pages 289–294, 2007.

[12] V. Degalahal, L. Li, V. Narayanan, M. Kandemir, and M. J. Irwin. Soft errors issues in low-power caches. *IEEE Trans. on Very Large Scale Integration (VLSI) Systems*, 13(10):1157–1166, Oct. 2005.

[13] A. Ejlali, M. T. Schmitz, B. M. Al-Hashimi, S. G. Miremadi, and P. Rosinger. Energy efficient seu-tolerance in dvs-enabled real-time systems through information redundancy. In *Proc. of the Int'l Symposium on Low Power and Electronics and Design (ISLPED)*, 2005.

[14] E. (Mootaz) Elnozahy, R. Melhem, and D. Mossé. Energy-efficient duplex and tmr real-time systems. In *Proc. of The* 23rd *IEEE Real-Time Systems Symposium*, Dec. 2002.

[15] D. Ernst, S. Das, S. Lee, D. Blaauw, T. Austin, T. Mudge, N. S. Kim, and K. Flautner. Razor: circuit-level correction of timing errors for low-power operation. *IEEE Micro*, 24(6):10–20, 2004.

[16] R. Ernst and W. Ye. Embedded program timing analysis based on path clustering and architecture classification. In *Proc. of The Int'l Conference on Computer-Aided Design*, pages 598–604, 1997.

[17] M. R. Garey and D. S. Johnson. *Computers and Intractability: A Guide to the Theory of NP-Completeness*. Mathematical Sciences Series. Freeman, 1979.

[18] P. Hazucha and C. Svensson. Impact of cmos technology scaling on the atmospheric neutron soft error rate. *IEEE Trans. on Nuclear Science*, 47(6):2586–2594, 2000.

[19] S. Irani, S. Shukla, and R. Gupta. Algorithms for power savings. In *Proc. of The* 14th *Symposium on Discrete Algorithms*, 2003.

[20] T. Ishihara and H. Yauura. Voltage scheduling problem for dynamically variable voltage processors. In *Proc. of The Int'l Symposium on Low Power Electronics and Design*, 1998.

[21] R.K. Iyer, D. J. Rossetti, and M.C. Hsueh. Measurement and modeling of computer reliability as affected by system activity. *ACM Trans. on Computer Systems*, 4(3):214–237, Aug. 1986.

[22] K. Jeffay and D. L. Stone. Accounting for interrupt handling costs in dynamic priority task systems. In *Proc. of the IEEE Real-Time Systems Symposium*, Dec. 1993.

[23] R. Jejurikar, C. Pereira, and R. Gupta. Leakage aware dynamic voltage scaling for real-time embedded systems. In *Proc. of the* 41st *Design automation conference*, 2004.

[24] A. R. Lebeck, X. Fan, H. Zeng, and C. S. Ellis. Power aware page allocation. In *Int'l Conference on Architectural Support for Programming Languages and Operating Systems*, 2000.

[25] C. L. Liu and James W. Layland. Scheduling algorithms for multiprogramming in a hard real-time environment. *J. ACM*, 20(1):46–61, 1973.

[26] R. Melhem, D. Mossé, and E. (Mootaz) Elnozahy. The interplay of power management and fault recovery in real-time systems. *IEEE Trans. on Computers*, 53(2):217–231, 2004.

[27] P. Pillai and K. G. Shin. Real-time dynamic voltage scaling for low-power embedded operating systems. In *Proc. of* 18th *ACM Symposium on Operating Systems Principles*, Oct. 2001.

[28] P. Pop, K.H. Poulsen, V. Izosimov, and P. Eles. Scheduling and voltage scaling for energy/reliability trade-offs in fault-tolerant time-triggered embedded systems. In *Proc. of the 5th IEEE/ACM Int'l Conference on Hardware/software codesign and System Synthesis (CODES+ISSS)*, pages 233–238, 2007.

[29] D. K. Pradhan. *Fault Tolerance Computing: Theory and Techniques*. Prentice Hall, 1986.

[30] S. Saewong and R. Rajkumar. Practical voltage scaling for fixed-priority rt-systems. In *Proc. of the* 9th *IEEE Real-Time and Embedded Technology and Applications Symposium*, 2003.

[31] C. Scordino and G. Lipari. A resrouce reservation algorithm for power-aware scheduling of periodic and aperiodic real-time tasks. *IEEE Trans. on Computers*, 55(12):1509–1522, 2006.

[32] K. Seth, A. Anantaraman, F. Mueller, and E. Rotenberg. Fast: Frequency-aware static timing analysis. In *Proc. of the* 24th *IEEE Real-Time System Symposium*, 2003.

[33] O. S. Unsal, I. Koren, and C. M. Krishna. Towards energy-aware software-based fault tolerance in real-time systems. In *Proc. of The Int'l Symposium on Low Power Electronics Design*, 2002.

[34] M. Weiser, B. Welch, A. Demers, and S. Shenker. Scheduling for reduced cpu energy. In *Proc. of The First USENIX Symposium on Operating Systems Design and Implementation*, Nov. 1994.

[35] F. Yao, A. Demers, and S. Shenker. A scheduling model for reduced cpu energy. In *Proc. of The* 36th *Annual Symposium on Foundations of Computer Science*, Oct. 1995.

[36] Y. Zhang and K. Chakrabarty. Energy-aware adaptive checkpointing in embedded real-time systems. In *Proc. of IEEE/ACM Design, Automation and Test in Europe Conference(DATE)*, 2003.

[37] Y. Zhang, K. Chakrabarty, and V. Swaminathan. Energy-aware fault tolerance in fixed-priority real-time embedded systems. In *Proc. of Int'l Conference on Computer Aided Design*, Nov. 2003.

[38] D. Zhu. Reliability-aware dynamic energy management in dependable embedded real-time systems. *to appear in ACM Trans. on Embedded Computing Systems; A preliminary version appeared in RTAS 2006*.

[39] D. Zhu and H. Aydin. Energy management for real-time embedded systems with reliability requirements. In *Proc. of the Int'l Conf. on Computer Aidded Design*, 2006.

[40] D. Zhu and H. Aydin. Reliability-aware energy management for periodic real-time tasks. Technical report, Dept. of Computer Science, Univ. of Texas at San Antonio, 2006. available at http://www.cs.utsa.edu/˜dzhu/papers/CS-TR-2008-005-zhu.pdf.

[41] D. Zhu, H. Aydin, and J.-J. Chen. Optimistic reliability aware energy management for real-time tasks with probabilistic execution times. In *to appear in the Proc. of the 29th IEEE Real-Time Systems Symposium (RTSS)*, 2008.

[42] D. Zhu, R. Melhem, and D. Mossé. The effects of energy management on reliability in real-time embedded systems. In *Proc. of the Int'l Conf. on Computer Aidded Design*, 2004.

[43] D. Zhu, R. Melhem, D. Mossé, and E.(Mootaz) Elnozahy. Analysis of an energy efficient optimistic tmr scheme. In *Proc. of the* 10th *Int'l Conference on Parallel and Distributed Systems*, 2004.

[44] D. Zhu, X. Qi, and H. Aydin. Priority-monotonic energy management for real-time systems with reliability requirements. In *Proc. of the IEEE International Conference on Computer Design (ICCD)*, 2007.

[45] D. Zhu, X. Qi, and H. Aydin. Energy management for periodic real-time tasks with variable assurance requirements. In *Proc. of the IEEE Int'l Conference on Embedded and Real-Time Computing Systems and Applications (RTCSA)*, 2008.

[46] J. F. Ziegler. Trends in electronic reliability: Effects of terrestrial cosmic rays. available at http://www.srim.org/SER/SERTrends.htm, 2004.